BULETINUL INSTITUTULUI POLITEHNIC DIN IAŞI

Volumul 66 (70)
Numărul 1-4

Secția
ŞTIINŢA ŞI INGINERIA MATERIALELOR

2020 **Editura POLITEHNIUM**

BULETINUL INSTITUTULUI POLITEHNIC DIN IAŞI
PUBLISHED BY
"GHEORGHE ASACHI" TECHNICAL UNIVERSITY OF IAŞI
Editorial Office: Bd. D. Mangeron 63, 700050, Iaşi, ROMANIA
Tel. 40-232-278683; Fax: 40-232-211667; e-mail: buletin-ipi@tuiasi.ro

Editorial Board

Scientific Board

BULETINUL INSTITUTULUI POLITEHNIC DIN IAŞI
BULLETIN OF THE POLYTECHNIC INSTITUTE OF IAŞI
Volumul 66 (70), Numărul 1-4 2020

Secția

ŞTIINŢA ŞI INGINERIA MATERIALELOR

SUMAR

BULETINUL INSTITUTULUI POLITEHNIC DIN IAŞI
BULLETIN OF THE POLYTECHNIC INSTITUTE OF IAŞI
Volume 66 (70), Number 1-4 2020

Section

MATERIALS SCIENCE AND ENGINEERING

CONTENTS

BULETINUL INSTITUTULUI POLITEHNIC DIN IAŞI
Publicat de
Universitatea Tehnică „Gheorghe Asachi” din Iaşi
Volumul 66 (70), Numărul 1-4, 2020
Secţia
ŞTIINŢA ŞI INGINERIA MATERIALELOR

AN X-RAY DIFFRACTION STUDY OF THERMOMECHANICAL PROCESSING EFFECTS ON LATTICE DISTORTION OF *α'* MARTENSITE, IN AN FeMnSiCr SHAPE MEMORY ALLOY

BY

MIHAI POPA[1], BOGDAN ISTRATE[2], BOGDAN PRICOP[1] and LEANDRU-GHEORGHE BUJOREANU[1,*]

[1]"Gheorghe Asachi" Technical University of Iași,
Faculty of Materials Science and Engineering, Iași, Romania
[2]"Gheorghe Asachi" Technical University of Iași,
Faculty of Mechanical Engineering, Iași, Romania

Received: January 20, 2020
Accepted for publication: February 25, 2020

Abstract. An Fe-28Mn-6Si-5Cr (mass. %) shape memory alloy (SMA) was subjected to both thermal and mechanical processing treatments. The former consisted in solution treatment at 1050°C, holding for 2, 4, 6, 8 and 10 hours and water quenching. The latter was an isothermal dynamic strain sweep by three point bending applied at room temperature (RT) with three bending frequencies, 1, 5 and 10 Hz. The fifteen thermomechanically processed specimens were analyzed by X-ray diffraction (XRD). Based on XRD patterns, the diffraction maxima corresponding to the component phases were identified, using crystallographic databases. After determining the real values of 2θ angles, of the main diffraction maxima, the interplanar spacings, d, were calculated and the unit cell constants, a, were determined for α' – body centered cubic martensite. Unit cell distortions, $\Delta a/a$, which were plotted as a function of solution treatment holding time and RT dynamic bending frequency, proved that the cell became tetragonal.

Keywords: FeMnSiCr shape memory alloy; holding time; DMA strain sweep; XRD patterns; lattice distortion.

*Corresponding author; *e-mail*: leandru-gheorghe.bujoreanu@academic.tuiasi.ro

1. Introduction

Fe-Mn-Si shape memory alloys (SMAs) became commercially available (Maki, 1998) both for their constrained recovery applications (Bujoreanu *et al*., 2008), as pipe coupling rings (Druker *et al*., 2014), rail fastening fishplates (Maruyama *et al*., 2008), pre-strained rods for concrete pre-stressing (Sawaguchi *et al*., 2006), embedded stripes for concrete beam curvature control (Shahverdi *et al*., 2016) and for their used as active elements in anti-seismic dampers (Sawaguchi *et al*., 2016). Based on polycrystalline Fe-(28-34)Mn-(4-6.5)Si (mass. %, as all chemical compositions will be listed hereinafter) SMAs, reported in 1987, which experienced an almost perfect SME (Murakami *et al*., 1987), quaternary and quintenary alloys were developed, as Fe-28Mn-6Si-5Cr (Otsuka *et al*., 1990) and Fe-14Mn-6Si-9Cr-5Ni (Moriya *et al*., 1991), respectively.

In Fe-Mn-Si SMAs, shape memory effect (SME) occurs during the thermally induced reversion of ε (hexagonal close-packed, hcp) stress-induced martensite (Kajiwara, 1999) to γ (face centred cubic, fcc) austenite. A second martensite, α' (body centred cubic, bcc) that reduces SME magnitude (Li *et al*., 2000), can be obtained after cooling high-Mn alloys (Bracke *et al*., 2006) or after the application of elevated stresses, where it is stress-induced at the intersection ε (hexagonal close-packed, hcp plates (Arruda *et al*., 1999).

Within previous work, the effects of thermomechanical processing of Fe-28Mn-6Si-5Cr SMA (comprising solution treatment holding time and dynamic three-point-bending frequency) were discussed, from the point of view of structural effects influencing storage modulus and internal friction variations, during isothermal strain sweep (Popa *et al*., 2019) and from the point of view of internal friction enhancement by the presence of ε - hcp martensite. One possible source for internal friction decrease, after long solution treatment holding times was assumed to be α' – bcc martensite that hinders the mobility of ε - hcp plates (Popa *et al*., 2021).

Aiming to perform deeper structural characterization, of above mentioned thermomechanical processing effects on lattice distortion of α' – bcc martensite at a 28Mn-6Si-5Cr SMA, the present paper employs X-ray diffraction (XRD) patterns to determine the experimental crystalline unit cell parameters in order to calculate lattice distortion.

2. Experimental Procedure

An Fe-28Mn-6Si-5Cr SMA alloy was melt, cut, hot rolled and solution treated at 1050°C for five holding times: 2, 4, 6, 8 and 10 h, with final water quenching (Popa *et al*., 2021). Several rectangular specimens (1 × 4 × 25 mm), in each of the five solution treatment states, were subjected to dynamic three-

point bending strain sweeps (DMA-SS-3PB) performed at room temperature (RT) with a DMA 242 E Artemis NETZSCH device, using a frequency of 1 Hz and an increasing strain amplitude. In each case, five RT-cycles were applied, during which strain increased between 0.01 and 0.09 %, as previously detailed (Popa *et al*., 2021).

The phasic structure was determined using an Expert PRO MPD diffractometer with Cu Kα radiation (λ_{Cu} = 1.540598 Å). XRD patterns were recorded on the significance region 2θ = 40-100^0 and maxima indexing for γ-fcc, ε-hcp and α′-bcc phases was performed using crystallographic databases 01-071-8288, 01-071-8285 and 00-034-0396, respectively. After indexing, the experimental values of 2θ angles ($2\theta_{exp}$) were determined from XRD plots and interplanar spacings, d_{hkl} were calculated based on Bragg law:

$$n\lambda_{Cu} = 2d_{hkl}\sin\frac{2\theta_{exp}}{2} \quad (1)$$

where n=1, for the first order of X-ray diffraction and h, k and l are Miller indices.

Using d_{hkl} values, the experimental values of lattice parameter of α' – bcc martensite, $a_{exp}^{\alpha'}$, were calculated from:

$$d_{hkl} = \frac{a_{exp}^{\alpha'}}{\sqrt{h^2+k^2+l^2}} \quad (2)$$

Finally, lattice distortion was determined with:

$$\frac{\Delta a}{a}\cdot 100 = \frac{a_{exp}^{\alpha'} - a_{th}^{\alpha'}}{a_{th}^{\alpha'}}\cdot 100 \quad (3)$$

where $a_{th}^{\alpha'}$ = 2.876 Å, according to 00-034-0396 crystallographic database.

3. Experimental Results and Discussion

The cumulated XRD plots, of the fifteen specimens under study are shown in Fig.1. It is obvious that only the structure of the specimens that were solution treated for 2 hours contains ε – hcp martensite.

The diffraction maxima, which were identified on the XRD plots and their corresponding *relative intensities*, according to crystallographic databases, have been:

(i) for γ-fcc austenite $(111)_\gamma$ – *999*, $(200)_\gamma$ – *420*, $(220)_\gamma$ – *172*, $(311)_\gamma$ – *158* and $(222)_\gamma$ – *43*;
(ii) for α' – bcc martensite $(110)_{\alpha'}$ – *100*, $(200)_{\alpha'}$ – *20*, $(211)_{\alpha'}$ – *50*, $(400)_{\alpha'}$ – *32* and $(622)_{\alpha'}$ – *53*;
(iii) for ε – hcp martensite $(101)\varepsilon$ – *999*, $(102)\varepsilon$ – *112* and $(103)\varepsilon$ – *98*.

The experimental values of diffraction maxima location, $2\theta_{exp}$, have been summarized in Table 1.

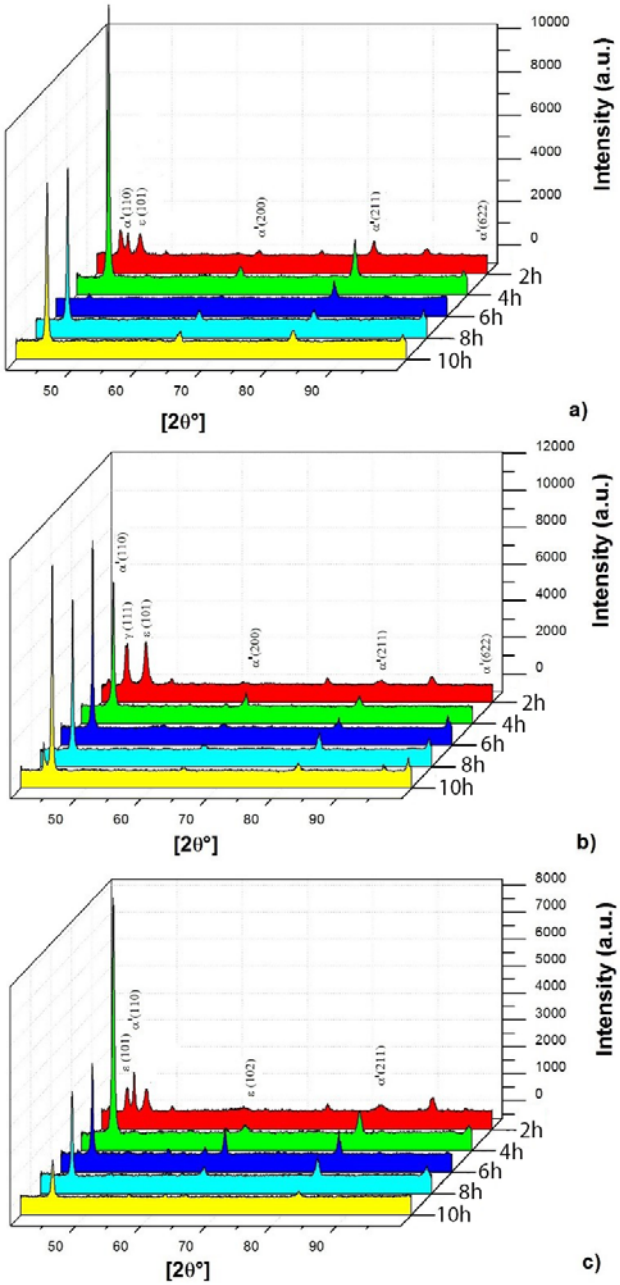

Fig. 1 – XRD plots of Fe-28Mn-6Si-5Cr SMA solution treated between 2 and 10 h, at 1050°C and subjected to five strain sweep cycles at different frequencies: (*a*) 1 Hz, (*b*) 5 Hz and (*c*) 10 Hz.

Table 1

Experimental Values of 2θ Angles Determined Based on the XRD Plots from Fig. 1, Using Crystallographic Databases

Theoretical values						Experimental values													
2θ (°)	I (a.u.)	Miller indices			Phase	Thermomechanical processing state: Holding time (hrs)/ DMA-SS-3PB frequency (Hz)													
		h	k	l		2/ 1	2/ 5	2/ 10	4/ 1	4/ 5	4/ 10	6/ 1	6/ 5	6/ 10	8/ 1	8/ 5	8/ 10	10/ 1	10/ 5	10/ 10
43.608	999	1	1	1	γ	43.5993	43.9669	43.9144											43.5336	
44.485	100	1	1	0	α'	44.7941		45.0305	44.9254	44.9123	44.9123	45.0305	44.8204	44.7941	44.8335	44.8598	44.781	44.7679	44.8335	44.9386
47.041	999	1	0	1	ε	46.6324	46.7768	46.9212												
50.795	420	2	0	0	γ	50.6371	50.7159	50.8472												
54.883	32	4	0	0	α'									56.3882						56.5589
62.128	112	1	0	2	ε			61.8241						62.113						62.3099
64.779	20	2	0	0	α'	64.8572			65.1723	65.2642		65.4218		65.1592	64.9228	64.9622	64.9622	65.2511		65.3561
74.681	172	2	2	0	γ	74.4686	74.5867	74.6393												82.6356
81.986	50	2	1	1	α'	82.4912			82.7144	82.6225	82.675	82.6225	82.5962	82.6093	82.6619	82.7144	82.4124	82.5962	82.5043	
83.634	98	1	0	3	ε			82.977												
90.673	158	3	1	1	γ	90.6188	90.6976	90.8945				90.435								
95.953	43	2	2	2	γ														95.6477	
99.676	53	6	2	2	α'							99.3373	99.3242		99.4292	99.5211	99.1929	99.3636	99.4555	

Since this study has been concerned on lattice distortion occurring in α' – bcc martensite, it is its main diffraction maximum, $(110)_{\alpha'}$ that was selected for further consideration.

Therefore, the values of $2\theta_{exp}$ angles, corresponding to $(110)_{\alpha'}$, were used for determining interplanar spacings, d_{110}, using Eq. (1), where λ_{Cu} = 1.540598 Å and experimental lattice constants, $a_{exp}^{\alpha'}$, determined with Eq. (2), where the Miller indices were considered h = 1, k = 1 and l = 0. All values are in Å.

Table 2 summarizes the values of d_{hkl} and $a_{exp}^{\alpha'}$, for α' – bcc martensite.

Table 2

Experimental Values of Interplanar Spacings d_{110} and Lattice Parameters, $a_{exp}^{\alpha'}$, Determined Based on $2\theta_{exp}$ Angles from Fig.1, for the Main Diffraction Maximum of α' – bcc Martensite (Å)

Holding time (hours)/ frequency (Hz)	d_{110}	$a_{exp}^{\alpha'}$
2/ 1	2.021718	3.501718
2/ 5	-	-
2/ 10	2.011652	3.484283
4/ 1	2.016114	3.492011
4/ 5	2.016671	3.492977
4/ 10	2.016671	3.492977
6/ 1	2.011652	3.484283
6/ 5	2.020593	3.499769
6/ 10	2.021718	3.501718
8/ 1	2.020033	3.498799
8/ 5	2.018909	3.496854
8/ 10	2.022279	3.50269
10/ 1	2.02284	3.503662
10/ 5	2.020033	3.498799
10/ 10	2.015552	3.491039

The values of experimental lattice parameters, $a_{exp}^{\alpha'}$, were further used to calculate lattice distortion with Eq. (3). The results are plotted in Fig. 2, as a function of holding time and strain sweep frequency.

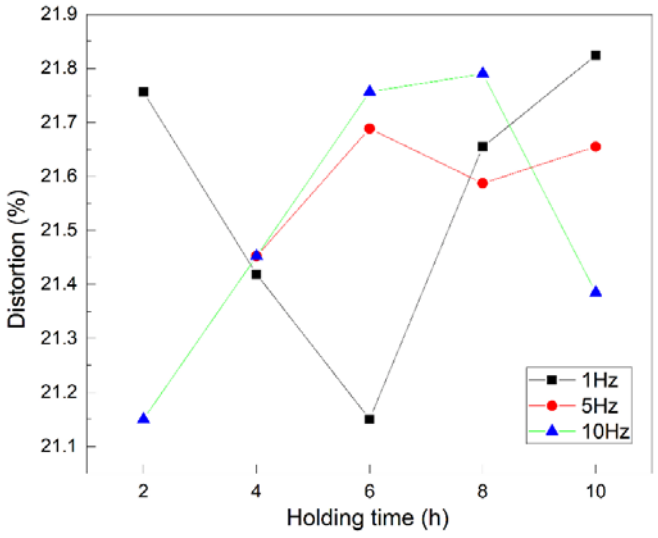

Fig. 2 – Lattice distortion of α' – bcc martensite *vs.* holding time and SS frequency.

Even if no monotonic variation tendencies of lattice distortion can be noticed, neither with the increase of holding time nor with that of strain sweep frequency, it is obvious that the parameter, $a_{exp}^{\alpha'}$, has been larger than $a_{th}^{\alpha'}$ = 2.876 Å in the case of fourteen amongst fifteen specimens. This proves that the bcc lattice became body centred tetragonal (bct) and the tetragonality degree ranges between 21.1 and 21.9%. These distortions could be an explanation for the low values of internal friction, observed in the specimens with large amounts of α' – bct martensite.

3. Conclusions

By means of XRD patterns, lattice distortions of α' – martensite were calculated. The results demonstrated that the unit cell was distorted, such as to become tetragonal, with a tetragonality degree of 21.5 ± 0.4%.

These third order stresses could be responsible for the low values of internal friction, observed in the Fe-28Mn-6Si-5Cr SMA under study.

The rather large tetragonality degree of α' – martensite could be a cause for blocking the mobility of ε – hcp martensite plates and an evidence for the change of martensite microstructure, from ε – hcp to α' – bct.

REFERENCES

Arruda G.J., Buono V.T.L., Andrade M.S., *The Influence of Deformation on the Microstructure and Transformation Temperatures of Fe–Mn–Si–Cr–Ni Shape Memory Alloys*, Mater. Sci. Eng. A, 273-275, 528-532 (1999).

Bracke L., Mertens G., Penning J., De Cooman B.C., Liebeherr M., Akdut N., *Influence of Phase Transformations on the Mechanical Properties of High-Strength Austenitic Fe-Mn-Cr steel*, Metall. Mater. Trans. A **37A**, 307-317 (2006).

Bujoreanu L.G., Dia V., Stanciu S., Susan M., Baciu C., *Study of the Tensile Constrained Recovery Behavior of a Fe-Mn-Si Shape Memory Alloy*, Eur. Phys. J. Special Topics, **158**, 15-20 (2008).

Druker A.V., Perotti A., Esquivel I., Malarría J., *A Manufacturing Process for Shaft and Pipe Couplings of Fe–Mn–Si–Ni–Cr Shape Memory Alloy*, Mater. Design, **56**, 878-888 (2014.).

Kajiwara S., *Characteristic Features of Shape Memory Effect and Related Transformation Behavior in Fe-Based Alloys*, Mat. Sci. Eng. A, 273-275, 67-88 (1999).

Li J.C., Zhao M., Jiang Q., *Alloy Design of Fe-Mn-Si-Cr-Ni Shape Memory Alloys Related to Stacking-Fault Energy*, Metall. Mater. Trans. A, **31**, 581-584 (2000).

Maki T., *Ferrous Shape Memory Alloys*, in Shape Memory Materials, (Otsuka K. and Wayman C.M., Eds.), Cambridge University Press, **117**, 1998.

Maruyama T., Kurita T., Kozaki S., Andou K., Farjami S., Kubo H., *Innovation in Producing Crane Rail Fishplate Using Fe-Mn-Si-Cr Based Shape Memory Alloy*, Mater. Sci. Technol., **24**, 908-912 (2008).

Moriya Y., Kimura H., Ishizaki S., Hashizume S., Suzuki S., Suzuki H., Sampei T., *Properties of Fe-Cr-Ni-Mn-Si (-Co) Shape Memory Alloys*, J. Phys. IV C **4**, 433-437 (1991).

Murakami M., Suzuki H., Nakamura Y., *Effect of Silicon on the Shape Memory Effect of Polycrystalline Fe-Mn-Si Alloys*, Trans. ISIJ **27**, B87 (1987).

Otsuka H., Yamada H., Maruyama T., Tanahashi H., Matsuda S., Murakami M., *Effects of Alloying Additions on Fe-Mn-Si Shape Memory Alloys*, Trans. ISIJ **30**, 674-679 (1990).

Popa M., Lohan N.-M., Popa F., Pricop B., Bujoreanu L.-G., *Holding-Temperature Effects on Thermally and Stress Induced Martensitic Transformations in an FeMnSiCr SMA*, Mater. Today: Proc. **19**, 956-962 (2019).

Popa M., Pricop B., Bujoreanu L.-G., *Structural Effects of Heat Treatment Holding-Time on Dynamic and Damping Behaviour of an Fe-28Mn-6Si-5Cr Shape Memory Alloy*, The Annals of "Dunărea de Jos" University of Galaţi, Fascicle IX, Metallurgy and Materials Science, vol. **5**, to be published, (2021).

Sawaguchi T., Kikuchi T., Ogawa K., Kajiwara S., Ikeo Y, Kojima M., Ogawa T., *Development of Prestressed Concrete Using Fe-Mn-Si-Based Shape Memory Alloys Containing NbC*, Mater. Trans. **47**, 580-583 (2006).

Sawaguchi T., Maruyama T., Otsuka H., Kushibe A., Inoue Y., Tsuzaki K., *Design Concept and Applications of FeMnSi-Based Alloys from Shape-Memory to Seismic Response Control*, Mater. Trans., **57**, *3*, 283 – 293, (2016).

Shahverdi M., Czaderski C., Motavalli M., *Iron-Based Shape Memory Alloys for Prestressed Near Surface Mounted Strengthening of Reinforced Concrete Beams*, Constr. Build. Mater. **112**, 28-38 (2016).

UN STUDIU PRIN DIFRACȚIE DE RAZE X A EFECTELOR PRELUCRĂRII TERMOMECANICE ASUPRA DISTORSIUNII REȚELEI MARTENSITEI α' A UNUI ALIAJ FeMnSiCr CU MEMORIA FORMEI

(Rezumat)

Un aliaj Fe-28Mn-6Si-5Cr (mass. %) cu memoria formei (AMF) a fost supus la tratamente de prelucrare termică și mecanică. Primul a constat din tratamente de punere în soluție la 1050°C, menținere timp de 2, 4, 6, 8 și 10 ore și călire în apă. Cel de-al doilea a fost o baleiere de amplitudine cu deformare dinamică izotermă aplicată la temperatura camerei (TC) cu trei frecvențe de încovoiere, 1, 5 și 10 Hz. Cele cincisprezece probe prelucrate termodinamic au fost analizate prin difracție de raze X (XRD). Pe baza modelelor XRD, au fost identificare maximele de difracție corespunzătoare fazelor componente, utilizând bazele de date cristalografice. După determinarea valorilor reale ale unghiurilor *2θ*, au fost calculate distanțele interplanare, *d*, și constantele celulei elementare, *a*, a martensitei α' – cubică cu volum centrat. Distorsiunile celulei elementare *Δa/a*, care au fost trasate în funcție de durata de menținere la tratamentul de punere în soluție și de frecvența de încovoiere dinamică la TC, au dovedit că celula a devenit tetragonală.

BULETINUL INSTITUTULUI POLITEHNIC DIN IAŞI
Publicat de
Universitatea Tehnică „Gheorghe Asachi” din Iaşi
Volumul 66 (70), Numărul 1-4, 2020
Secţia
ŞTIINŢA ŞI INGINERIA MATERIALELOR

DETERMINATIONS BY MEASUREMENTS OF RADIO FREQUENCY ELECTROMAGNETIC FIELD LEVELS GENERATED BY DVB-T2 TECHNOLOGY. ASSESSMENT OF COMPLIANCE WITH ROMANIAN EXPOSURE NORMS FOR THE GENERAL AND OCCUPATIONAL POPULATION

BY

ANDREI IONUŢ MIHĂILĂ, ANIŞOARA CORĂBIERU* and GHEORGHE BĂDĂRĂU

“Gheorghe Asachi” Technical University of Iași,
Faculty of Materials Science and Engineering, Iași, Romania

Received: January 20, 2020
Accepted for publication: April 21, 2020

Abstract. The study represents the determination of the electromagnetic field (EMF) levels generated by the new DVB-T2 digital television transmission technology in the Iași urban agglomeration, as well as the verification of the conformity of the values obtained with the exposure limit values (ELV) of the norms in force for occupational exposure. The exposure limit values imposed by the regulation in force are based on the recommendations of the International Commission on Non-Ionizing Radiation Protection (ICNIRP). Between February 14th-19th, 2020, a number of 70 field level determinations were performed, in different locations within the city of Iasi (Romania) and in its immediate vicinity. The analyzed electromagnetic field is generated by a transmitter antenna located at a height of approximately 184 meters, at the top of the DRTV tower (ROU32 coverage area) located on Repedea hill, Pietrăria locality. A measurement system consisting of a broadband sensor and a spectrum analyzer was used, both Aaronia brand, and the measurement methodology is based on the European standard EN 50492: 2008 „Basic standard for the in-situ measurement of

*Corresponding author; *e-mail*: anisoara.corabieru@academic.tuisi.ro

electromagnetic field strength related to human exposure in the vicinity of base stations". The results showed that field levels, both in terms of the general population and the occupational population, are well below the limits imposed by the national norms.

Keywords: occupational exposure; general exposure; measurements; electromagnetic field; DVB-T digital television.

1. Introduction

Electromagnetic pollution is invisible, odorless and generally difficult to perceive for the human senses, which is why it is so ignored compared to other "traditional" types of pollution.

In recent decades, we have witnessed an accelerated emergence and an increasing use of new communication technologies, especially in densely populated areas.

We are all exposed every day to a complex mixture of natural and artificial electromagnetic fields (EMFs), both at work and in public spaces or at home.

This aspect entails the need to determine EMF levels, as well as to investigate the negative effects they can have on human health and the environment.

EMF can act on humans in two ways, indirectly and directly. Indirect effects refer to the fact that the presence of an object in a region with a strong EMC can turn it into a projectile, thus becoming a source of danger to human health and integrity.

These objects can be external to the human body such as metal or ferromagnetic parts, but they can also be inside the body such as implants, whether we are talking about passive ones (metal rods) or active implants (such as pacemakers).

With the advent of new radiocommunication technologies, the study of the direct influence of EMF on living organisms has been of great concern to the global scientific community.

Countless studies have been performed taking into account the characteristics of EMFs in different regions around the generating source, exposure time, body position, health status of exposed persons, age.

However, the only scientifically established direct effects refer to short-term exposure: non-thermal effects - nervous and muscular stimulation upon exposure to low-frequency EMF, and thermal effects caused by the absorption of high-frequency energy

The level of exposure to radio frequency EMF is constantly changing and depends directly on several factors such as the number of emitting sources, their emission power, frequency and last but not least the distance.

Regarding the distance from the generating source, two field areas can be distinguished (near and far). In the nearby field area, EMFs have an inhomogeneous structure, very complex and unpredictable.

In the immediate vicinity of the generating source, the electric (E) and magnetic (H) field vectors are out of phase, which makes them have a reactive and not radiative characteristic necessary for propagation.

As we move away from the source, the fields (E) and (H) begin to align and move from the reactive to the radiative characteristic. This transition region is also known as the Fresnel area.

Because in the Fresnel area, EMFs have not completely transitioned, the shape of the radiation model still varies with distance, and the determination of EMF levels is very difficult to achieve. In the remote field area, the EMF structure is relatively simple, the fields (E) and (H) are orthogonal to each other in the direction of propagation, and the determination of EMF levels is relatively easy.

2. The Aim of the Study

The aim of the study is to determine the EMFs levels generated by the new digital television transmission technology, the DVB-T2 standard, in the Iaşi urban agglomeration and to assess the conformity of the values obtained with the exposure limit values (ELV) of the national regulations in force.

3. DVB-T2 Technology

DVB-T2 (https://dvb.org/about/), is a European standard for second generation digital terrestrial television transmission that replaces the old standard of analogue transmission. Fig. 1 shows the signal coverage DVB-T2 for Romania, in December 2020.

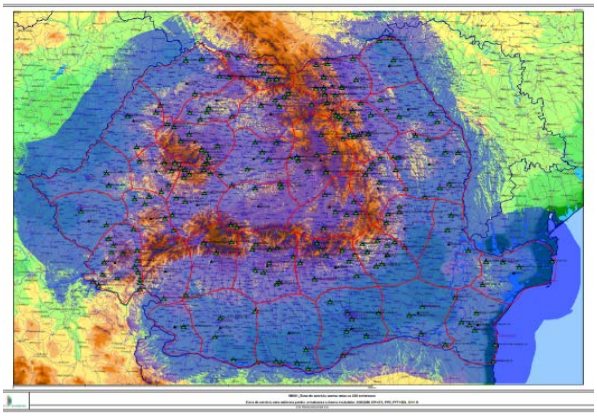

Fig. 1 – The map of signal coveraje DVB-T2, for Romania, December 2020, source http://www.radiocom.ro/poze/dvb-t2/MUX1_Zona%20de%20serviciu% 20228%.

The technology was implemented in Romania during 2015-2017 based on the agreement (RRC 06) signed in 2006 in Geneva, at the Regional Conference on Radiocommunications of the International Telecommunication Union (ITU).

More information about the DVB-T2 standard, the strategy and the implementation of the technology in Romania, can be found on the following sites: http://search.itu.int/history/HistoryDigitalCollectionDocLibrary/4.129.43.; https://www.comunicatii.gov.ro/; http://www.radiocom.ro/despre-noi/DVB_T2/#).

3.1. The Generator Source

DVB-T2 transmissions appear in the ultra high frequency band (UHV) and are made with the help of high power main transmitters (antennas), located at considerable heights with wide terrestrial coverage.

Fig. 2 – Repedea hill antenna – the electromagnetic field source, placed in Pietrăria, Iași County.

For the "shaded" areas, the transmissions are made with the help of repeaters that take the signal from the main transmitter and retransmit it to the areas without coverage.

The DVBT-2 signals analyzed in this study come from a transmitter with a power of 2.5 kW, located at the top of the telecommunications tower (approximately 186 m from the ground) in Pietrăria, Iași, shown in Fig. 2.

The broadcast is made on channel 43, it has the B Signal bandwidth is 8 MHz with the center of the CF band = 650 MHz.

3.2. Measurement System

Taking into account the signal characteristics and the intended purpose, we used a measurement system consisting of a SPECTRAN HF-60105

spectrum analyzer with a working range between 1 MHz and 9.4 GHz and a Bico LOG 20300 broadband sensor (20 MHz - 3 GHz), both from the German manufacturer Aaronia AG.

3.2.1. System Setting

Max Hold mode: Medium Square Root (RMS); B signal = 8 MHz; RBW bandwidth resolution = 5 MHz; VBW video bandwidth = 50 MHz (full); A Sample Time test time of 250 ms; Sweep Time scan time = 750 ms; CF band center = 650MHz; Scanned range = 20 MHz between 640 MHz and 660 MHz.

3.3. Measured Points

The measurement points were chosen taking into account two criteria in terms of their relationship to the source: direct, unshaded (LOS) and shaded (NO LOS); the principle for LOS is shown in Fig. 3 and for NO-LOS in Fig. 4.

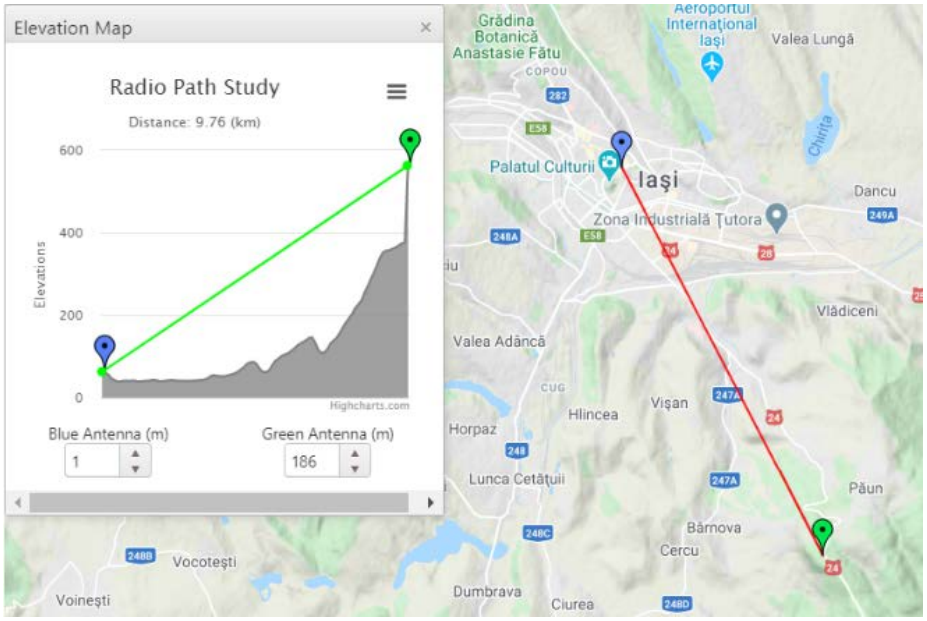

Fig. 3 – LOS – unshadowed zone.

The measuring points were divided into 4 lots. Lot 1 - in the vicinity of the transmitter at a distance of approximately 160 m; Lot 2 - on the horizon line from the perspective of the man at the base of the transmitting tower; Lot 3 and 4 - within the city of Iași. Fig. 5 shows the measuring points on the map.

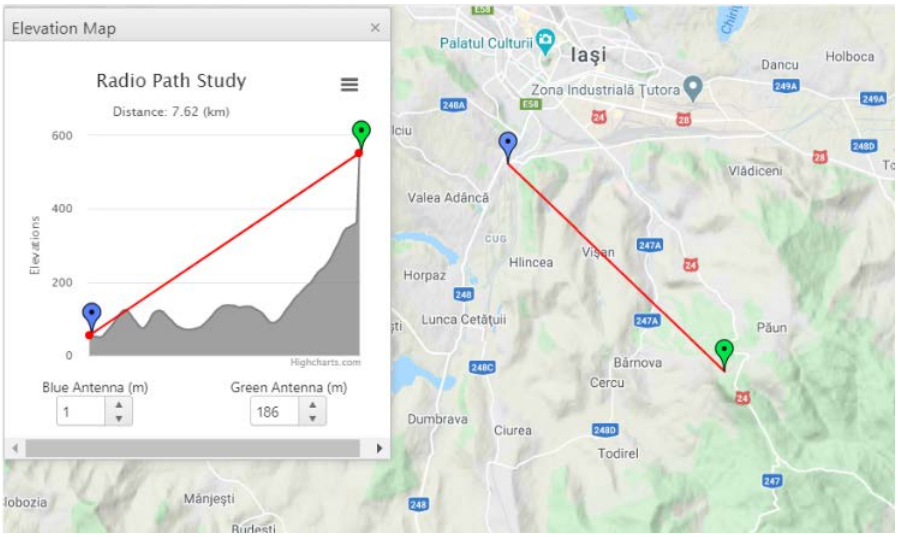

Fig. 4 – No LOS – shadowed zone.

Table 1

Measurement Points

LOS	No LOS	Sign color on the map
Lot 1		Red
Lot 2		Green
Lot 3		Yellow
	Lot 4	Blue

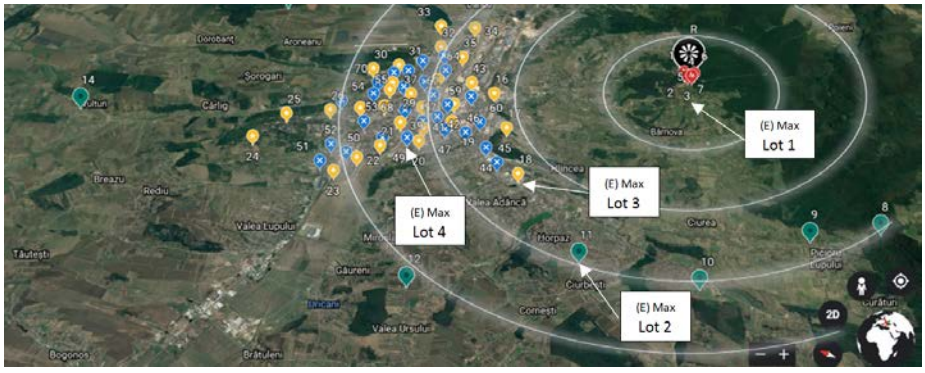

Fig. 5 – Measurement points marked with colors.

3.3.1. Measurement of Points

In each location the maximum power of the P [dBm] signal was determined over a period of 6 min, in three orthogonal directions (x, y, z), at a

height from the ground of 1.5 m according to [ComReg 08 / 51R2 Page 8 of 119]. Throughout the sampling period, a distance of at least 0.5 m from the sensor was maintained in order to avoid field disturbance. The data were recorded in an Excel table, correction formulas were applied taking into account the cable losses as well as the antenna factor, they were converted into the intensity of the electric field (E_Z, E_Y, E_Z), and the total reconstruction was performed for each point apart $E_{Total} = \sqrt{E_x^2 + E_y^2 + E_z^2}$ [REC0204 Item 4.7 Analog / Digital wide-band broadcast (TV, T-DAB, DVB-T, ...)]. The measurements were performed between 14th -19th February 2020 on a total number of 70 measurement points.

4. Regulations

4.1. Internationally

The recommendations of the International Commission on Non-Ionizing Radiation Protection (ICNIRP) are the most widely used globally either directly or as a basis for national regulations. The ICNIRP standard divides the population exposed to EMF into two categories: the general population and the occupational population.

Table 2
Exposure Limits (Basic Restrictions)

Type of exposure	Frequency range	Current density for head and trunk (mA/m^2) (RMS)	SAR Entire body	SAR Locallised head and trunk	SAR Locallised on members
Occupational	<1 Hz	40	-	-	-
	1 – 4 Hz	40/f	-	-	-
	4 Hz – 1 kHz	10	-	-	-
	1 – 100 kHz	f/100	-	-	-
	100 kHz –10 MHz	f/100	0.4	10	20
	10 MHz – 10 GHz	-	0.4	10	20
General	<1 Hz	8	-	-	-
	1 – 4 Hz	8/f	-	-	-
	4 Hz – 1 kHz	2	-	-	-
	1 – 100 kHz	f/500	-	-	-
	100 kHz – 10 MHz	f/500	0.08	2	4
	10 MHz – 10 GHz	-	0.08	2	4
*Note:	f – frequency expressed in Hertz SAR values are for a time of exposure of 6 min The mass to mediate SAR localised head, trunk and members 10 g of tissue.				

The exposure limits present in the recommendation are the quantities most closely related to adverse biological effects. These include amounts to be

determined in human tissue. Their determination must take into account the type of radiant source, the frequency of operation or the duration of exposure.

The basic restrictions presented in Table 2 are established so as to take into account uncertainties related to individual sensitivity, environmental conditions, age and health status of the population, are based on extensive scientific research and are internationally recognized.

4.1.1. Reference Levels

The reference levels for human exposure to electric, magnetic and electromagnetic fields are derived from the basic restrictions, using the realistic hypothesis of the most unfavorable case regarding exposure.

If the reference limits are met, then the basic restrictions will also be met; if the reference levels are exceeded, this does not necessarily mean that the basic restrictions are exceeded.

This type of approach shows a conservative position regarding compliance with reference levels. In Table 3 presents the Reference Level Limits as defined by the ICNIRP standard.

Table 3

Reference Levels for Human Exposure to Electric Fields

Type of exposure	Frequency range	Intensity of electrical field (V/m)	Intensity of magnetic field (A/m)	Power density of the equivalent plane wave (W/m^2)
Occupational	< 1 Hz	-	$1.63*10^5$	-
	1 – 8 Hz	20 000	$1.63 * 10^5 / f^2$	-
	8 – 25 Hz	20 000	$2 * 10^4 / f$	-
	0.025 – 0.82 kHz	500 / f	20 / f	-
	0.82 – 65 kHz	610	24.4	-
	0.65 – 1 MHz	610	1.6 / f	-
	1 – 10 MHz	610 / f	1.6 / f	-
	10 – 400 MHz	61	0.16	10
	400 – 2000 MHz	$3 * f^{1/2}$	$0.008 * f^{1/2}$	f / 40
	2 – 300 GHz	137	0.36	50
General	< 1 Hz	-	$3.2 * 10^4$	-
	1 – 8 Hz	10 000	$3.2 * 10^4 / f^2$	-
	8 – 25 Hz	10 000	4000 / f	-
	0.025 – 0.8 kHz	250 / f	4 / f	-
	0.8 – 3 kHz	250 / f	5	-
	3 – 150kHz	87	5	-
	0.15 – 1 MHz	87	0.73 / f	-
	1 – 10 MHz	$87 / f^{1/2}$	0.73 / f	-
	10 – 400 MHz	28	0.073	2
	400 – 2000 MHz	$1.375 * f^{1/2}$	$0.0037 * f^{1/2}$	f / 200
	2 – 300 GHz	61	0.16	10
* Note: For frequencies between 100 kHz and 10 GHz, the exposure time is 6 min				

4.2. At European Level

From the point of view of human protection regarding the limitation of EMF exposure, the European Commission has issued two documents, one for the general population and one for the occupational population. Both documents are based on ICNIRP recommendations.

The European Council Recommendation 1999/519 / EC concerning the limitation of exposure of the general population to electromagnetic fields (from 0 Hz to 300 GHz) is a non-binding document, but comes as a recommendation to Member States for the implementation in national legislation of a legislative forms of population protection exposed to EMF of radio frequency.

European Directive 2013/35 / EU on minimum health and safety requirements for the exposure of workers to the risks posed by physical agents (electromagnetic fields) is a binding document, with all EU Member States being required to transpose it into national law by July 1, 2016.

4.3. Nationally

The reaction at national level in Romania came on September 29th, 2006, when the Ministry of Public Health issued Order no. 1193 for the adoption of the "Rules on limiting the exposure of the general population to EMF from 0 Hz to 300 GHz", taking over almost entirely the European Council Recommendation 1999/519 / EC. Regarding the occupational population, a Government Decision no. 520 of 2016 which fully took over the European Directive 2013/35 / EU.

4.4. Similar Studies

A number of studies on radio frequency (RF) electromagnetic field (EMF) exposure from terrestrial television transmission have been published in recent decades.

A study conducted in over 300 locations located in the residential areas of Munich and Neurnberg (Germany), was based on determining the EMC levels before and after the transition from analog to digital. The study shows a significant increase in electric field strength (E), but nevertheless, the levels recorded are still well below the ICNIRP reference limits (Schubert *et al*., 2007).

In Belgium, the Netherlands and Sweden, a study was conducted to estimate the level of exposure to radio frequency electromagnetic fields generated by wireless communication technologies, in 6 different exposure environments: Rural, Residential, Urban, Suburban, Interior offices, and industrial.

According to this study, published in 2012, except for GSM technology, the level of electromagnetic fields generated by the DVB-T system was higher than the level of fields generated by other technologies, and the highest value of

electric field strength (E), respectively 1.65 V/m, was determined in the Urban area in the immediate vicinity of the generating source (Wout *et al*., 2012).

A 2013 study treats human exposure to the electromagnetic field generated by a DVB-T transmitter in the center of the Croatian city of Zagreb.

EMC measurements were performed in several key locations and compared with the values obtained by theoretical calculations, and the results showed similar values between those determined by numerical calculations and those determined by in-situ measurements. The electric field strength (E) does not exceed at any point the value of 0.3 V/m (Juriev-Sudac and Krešimir, 2013).

Similar results were obtained following a study conducted in 2016 and which consisted of performing 20 measurements around an EMC source located in the center of the Thai capital, Bangkok (Suwansukho, 2016).

The maximum values obtained did not exceed 80 dBμV, which represents a value of electric field strength (E) of maximum 0.450 V/m.

A similar study was done in Iasi, in 2016 (Luncă *et al*., 2016), when the DVB-T2 transmission was made on channel 25 (506 MHz). The research involved determining the intensity of the electric field (E) in 80 measuring points: 62 in different areas of the city of Iasi and 18 in the vicinity of the generating source, DVB-T2 antenna at the top of the Pietrăria tower.

The highest value of the electric field strength (E) of the total measurements performed was 0.382 V/m, recorded at a point 150 meters from the tower. In the urban area, the maximum value recorded was 0.096 V/m.

We can therefore observe, by comparison, a slight increase in the intensity of the electric field (E) following the change of the transmission from channel 25 (506 MHz) to channel 43 (650 MHz).

A report published in 2015 by the Scientific Committee for Emerging and Newly Identified Health Risks (SCENIHR) of the European Commission analyzes several studies in recent decades and, according to the authors, although current EMC levels due to television transmission are much higher compared to those recorded in the 1980s, with the migration to digital television, in some areas, there were decreases in exposure levels (https://ec.europa.eu/health/scientific_committees/emerging/docs/).

5. Results Obtained and Discussion

The highest value of the electric field strength (E) of the total measurements performed was recorded in lot 1 of measurements, point 3, *i.e*. in the immediate vicinity of the EMF generating source. The value is 0.481 V/m which represents 1.37% of the reference limit (E) for the general population (Order no. 1193/2006) and 0.63% of the reference limit (E) for the occupational population (GD no. 520/2016).

Fig. 6 – Maximum values measured on map.

In lot 2, the maximum value of the measured electric field intensity (E) was in point 11, on the ring road between Ciurbești and Horpaz localities, at a distance of 8.48 km from the EMF source. The value determined at this point was 0.115 V / m, which represents 0.33% of the reference limit for the general population and 0.15% of the occupational one, Fig. 6. A graphic representation of the degree of exposure is given in Fig. 7.

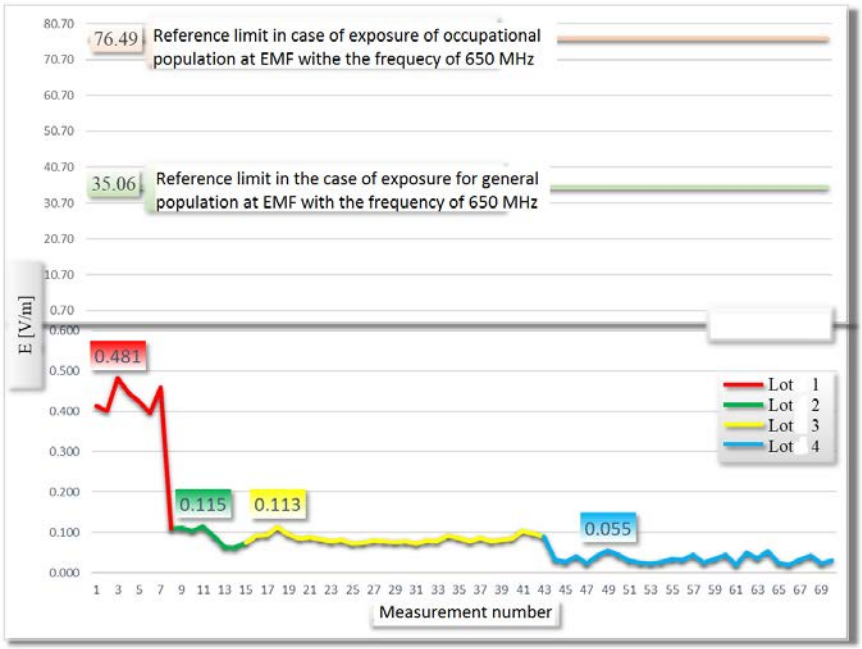

Fig. 7 – Graphic representation of the degree of exposure to EMF.

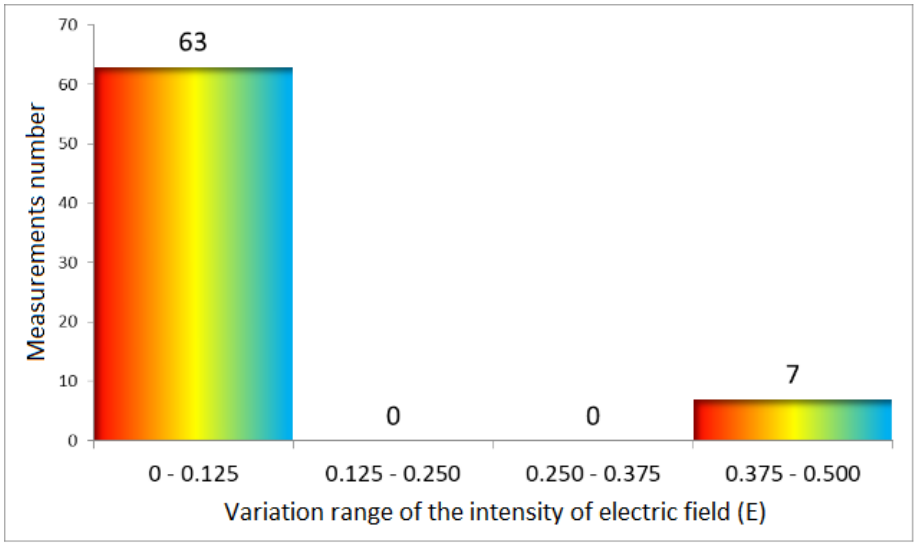

Fig. 8 – Variation range of the measured intensity of electric field *vs.* measurements number.

In lot 3, the highest intensity value (E) was determined in point 18, end CUG - Tehnopolis at a distance of 7.31 km from the source and is 0.113 V/m which represents 0.32% of the reference limit for general population and 0.15% of the limit for the occupational population.

In lot 4, as expected because the visibility between the source and the measuring points is obstructed either by relief, or by vegetation, or by buildings, we obtained the lowest values of the electric field intensity (E). Practically, the highest value obtained in this set of measurements, was registered in point 49 of the Voievozilor Square and is 0.055 V/m which represents 0.16% of the limit for the general population and 0.07% of that for the occupational population.

The variation range of the measured intensity of the electri field versus the measurements number is shown in Fig. 8.

6. Conclusions

According to the results of this study, the level of EMF exposure is well below the reference limits. Only 10% of the total number of measurements reached the threshold of 1% of the reference limit for the general population, respectively 0.5% of the limit for the occupational one. The maximum value of the electric field intensity (E) was 0.481 V/m which corresponds to a percentage

of the reference limit of only 1.37% (general population) and 0.63% (occupational population).

REFERENCES

Juriev-Sudac L., Krešimir M., *Exposureto Electromagnetic Fieldfrom DVB-T Transmitter University of Zagreb*, DOI: 10.1109/SoftCOM.2013.6671874, Faculty of Electrical Engineering and Computing, Department of Wireless Communications, Zagreb, Croatia (2013).

Luncă E., Sălceanu A., Ursache S. et al., *Evaluation of EMF Exposure from Digital Terrestrial Television Transmitters*, Conference: 21st IMEKO TC4 International Symposiumand 19th International Workshop on ADC Modelingand Testing Understanding the World Trough Electricaland Electronic Measurement, Budapest, Hungary (2016).

Schubert M., Bornkessel C., Wuschek M., Schmidt P., *Exposure of the General Public to Digital Broadcast Transmitters Compared to Analogue Ones*, doi.org/10.1093/rpd/ncm337, 2007.

Suwansukho N., *Experimental Study of DVB-T2 in Thailand*, DOI: 10.1109/ICSEC.2016.7859933, Faculty of Engineering King Mongkut's Institute of Technology Ladkrabang, Bangkok, Thailand (2016).

Wout J., Verloock L., Goeminne F. et al., *Assessment of RF Exposure from Emerging Wireless Communication Technologies in Different Enviroments*, Health Physics, **102**, DOI: 10.1097/HP.0b013e31822f8e39, Department of Information Technology, Ghent University, Belgium, 2012, https://www.academia.edu/31383555/Assessment_of_RF_Exposures_from Emerging_Wireless_CommunicationTechnologies_in_Different_Environments

** Aaronia AG, Handheld Spectrum Analyzer Series SPECTRAN® V4, Datasheet, 2014, https://downloads.aaronia.com/datasheets/analyzers/V4/Aaronia_ Spectran_V4 _HF_60100_sweep_analyzer.pdf.

** Aaronia AG, Biconical EMC Broadband Antennas - BicoLOG Series, Datasheet, 2014, https://www.batronix.com/files/Aaronia-AG/Antennas/BicoLOG-EMV-Datasheet.pdf.

** CCR - Commision for Communications Regulations, Programme of Measurement of Non-Ionising Radiation Emissions. Methodology for the Conduct of Surveys to Measure Non-Ionizing Electromagnetic Radiation from Transmitter Sites, Document No. 08/51R2, 2014, http://www.comreg.ie/_fileupload/publications/ ComReg0851R2.pdf.

** Directiva – DE 2013/35/UE, Directiva 2013/35/UE a Parlamentului European şi a Consiliului privind cerinţele minime de sănătate şi securitate referitoare la expunerea lucrătorilor la riscuri generate de agenţii fizici (câmpuri electromagnetice) [a douăzecea directivă specială în sensul articolului 16 alineatul (1) din Directiva 89/391/CEE] şi de abrogare a Directivei 2004/40/CE, Jurnalul Oficial al Uniunii Europene, 2013, https://eur-lex. europa.eu /legal-content/RO/TXT/PDF/?uri=CELEX:32013L0035 .

** Final Acts of the Regional Radiocommunication Conference for Planning of the Digital Terrestrial Broad Casting Service in Parts of Regions 1 and 3, in the

Frequency Bands 174-230 MHz and 470-862 MHz (RRC-06) Geneva, 15 May - 16 June 2006 http://search.itu.int/history/HistoryDigitalCollection Doc Library/4.129.43.en.100.pdf

⁎*⁎ Guvernul României (2016), HG 520/2016 privind cerințele minime de securitate și sănătate referitoare la expunerea lucrătorilor la riscuri generate de câmpuri electromagnetice, Monitorul Oficial al României, partea I, no. 576 din 28.07.2016, http://www.mmuncii.ro/j33/images/Documente/Legislatie/HG520-2016.pdf.

⁎*⁎ Ministerul Sănatatii Publice (2006), Ordin de Ministru nr. 1193/2006 pentru aprobarea Normelor privind limitarea expunerii populației generale la câmpuri electromagnetice de la 0 Hz la 300 GHz, Monitorul Oficial al României, no. 895 din 03.11.2006, https://www.ancom.ro/uploads/links_files/ Odinul_1193_2006_norme.pdf.

⁎*⁎ Recomandarea CEPT/ECC/REC/(02)04 privind metodele de măsurare a radiațiilor electromagnetice neionizante (9kHz – 300 GHz), https://docdb.cept.org /download/ fa5b1c03-0a47/ REC0204.PDF.

⁎*⁎ Recomandarea Consiliului European – REC 1999/519/EC, Council Recommendation on the Limitation of Exposure of the General Public to Electromagnetic Fields (0Hz – 300 GHz), Official Journal of the European Communities, 1999, https://eur-lex.europa.eu/LexUriServ/LexUriServ.do?uri=OJ:L:1999:199: 0059: 0070: EN:PDF.

⁎*⁎ Scientific Committee on Emerging and Newly Identified Health Risks SCENIHR Opinion on Potential Health Effects of Exposure to Electromagnetic Fields (EMF), Doi: 10.2772/75635, 2015, https://ec.europa.eu/health/scientific committees/ emerging/docs/ scenihr_o_041.pdf

⁎*⁎ Standard ICNIRP – International Commission on Non-Ionizing Radiation Protection, Guidelines for Limiting Exposure To Electromagnetic Fields (100 kHz up to 300 GHz), Health Physics, 118(5):483-524, 2020, https://www.icnirp.org/cms/ upload/publications /ICNIRPrfgdl2020.pdf .

⁎*⁎ Strategia privind tranziția de la televiziunea analogică terestră la cea digitală terestră și implementarea serviciilor multimedia digitale la nivel național https://www.comunicatii.gov.ro/wp-content/uploads /2016/02/ Strategie -TV-digitala-terestra.pdf

http://www.radiocom.ro/despre-noi/DVB_T2/#

https://dvb.org/about/

DETERMINĂRI PRIN MĂSURĂTORI ALE NIVELURILOR DE CÂMP ELECTROMAGNETIC DE RADIOFRECVENȚĂ GENERAT DE TEHNOLOGIA DVB-T2. EVALUAREA CONFORMITĂȚII CU NORMELE ROMÂNEȘTI DE EXPUNERE PENTRU POPULAȚIA GENERALĂ ȘI OCUPAȚIONALĂ

(Rezumat)

Studiul reprezintă determinarea nivelurilor de câmp electromagnetic (CEM) generat de noua tehnologie de transmisie a televiziunii digitale DVB-T2 în aglomerarea

urbană Iași, precum și verificarea conformității valorilor obținute cu valorile limită de expunere (VLE) din normele în vigoare pentru expunerea ocupațională şi cea generală. VLE-urile impuse de norme au la baza recomandările Comisiei Internaționale pentru Protecția împotriva Radiațiilor Neionizante (ICNIRP). În perioada 14-19 Februarie 2020 au fost efectuate un număr de 70 de determinări ale nivelului de câmp, în diferite locații de pe raza orașului Iași (Romania) şi în imediata vecinătate a acestuia. Câmpul electromagnetic analizat este generat de o antenă emițător amplasată la o înălțime de aproximativ 184 de metri, în vârful turnului DRTV (aria de acoperire ROU32) aflat pe dealul Repedea, localitatea Pietrăria. S-a utilizat un sistem de măsurare format dintr-un senzor de bandă largă și un analizor de spectru, ambele marca Aaronia, iar metodologia de măsurare se bazează pe standardul european EN 50492:2008 „Basic standard for the in-situ measurement of electromagnetic field strength related to human exposure in the vicinity of base stations”. Rezultatele au arătat faptul că nivelele de câmp, atât în ceea ce privește populația generală cât şi cea ocupațională, sunt mult sub limitele impuse de normele naționale.

BULETINUL INSTITUTULUI POLITEHNIC DIN IAŞI
Publicat de
Universitatea Tehnică „Gheorghe Asachi” din Iaşi
Volumul 66 (70), Numărul 1-4, 2020
Secţia
ŞTIINŢA ŞI INGINERIA MATERIALELOR

OCCUPATIONAL HEALTH AND SAFETY RISKS IN DENTAL OFFICES IN THE CONTEXT OF COVID-19 PANDEMIC

BY

DORU COSTIN DARABONT[1], ANCA-MONICA DARABONT[2] and COSTICĂ BEJINARIU[3,*]

[1]National Research and Development Institute of Occupational Safety "Alexandru Darabont", București, Romania
[2]Romanian Dental Association of Private Practitioners, București, Romania
[3]"Gheorghe Asachi" Technical University of Iași,
Faculty of Materials Science and Engineering, Iași, Romania

Received: October 5, 2020
Accepted for publication: November 18, 2020

Abstract. The activity performed by professionals in dental offices is characterised by specific occupational health and safety (OHS) risks, generated by the equipment used and medical procedures applied as well as by some health aspects of the patients. A well performed risk assessment is a necessary condition to establish adequate preventive and protective measures and to provide a proper training to the employees. Moreover, the COVID-19 pandemic generates new risks for OHS in dental offices and amplifies some of the pre-existing risks. The paper focuses on changes determined by the pandemic on the OHS risks and on the preventive and protective measures necessary to be adopted to reduce the impact of these changes on dental offices professionals.

Key words: occupational health and safety; risk assessment; dental office; COVID-19 pandemic.

*Corresponding author; *e-mail*: costica.bejinariu@tuiasi.ro

1. Introduction

As any other professional activity, the activity performed by the medical personnel in dental offices involves OHS risks. In this case, the risks are generated mainly by the specific equipment and medical procedures applied for treatment, but also by the patients having different contagious diseases, including COVID-19.

The first step for ensuring the safety and protecting the health of medical personnel in dental offices is to perform a proper risk assessment, taking into consideration all the components of the work system, respectively, operator (human), work task, means of production (consisting, in this case, of hand tools, dental unit, sterilizing equipment, raw materials, facilities) and work environment (Pece 2010; Darabont *et al*., 2019). Also, the OHS Law no.319/2006 and its methodological norms of applying require the employer to ensure the performing of hazard identification and risk assessment for workplaces, considering specifically each components of the work system (Law no. 319/2006; Government Decision no.1425/2006).

Generally, the employers observe the obligation to assess the risks and to adopt preventive and protective measures to keep the identified risks under control. However, the COVID-19 pandemic has induced significant changes in the structure and level of the OHS risks for all workplaces and particularly, for dental offices. In the dental offices case, these changes were determined, mainly, by the raised probability to provide treatment to contagious patients infected with SARS-CoV-2, even they are symptomatic or not. This potential situation determines new risks for medical personnel, for example, the risk of being infected with the coronavirus, but also change de level of other previously existing risks. For example, the risk level of performing aerosol-generating procedures was assessed as "*High*" before pandemic, but is changed to "*Very high*" in case of treating a known or suspected COVID-19 patient (American Dental Association, 2021). Thus, a certain procedures, *e.g.* dental scaling, which was assessed to an acceptable risk level before pandemic, becomes unsafe for the health of medical staff and the employer or authorities should ban this procedure during pandemic, especially it is not a medical emergency.

Considering these changes, the risk assessment should be reviewed in the context of COVID-19 pandemic, and new protective and preventive measures should be established and implemented. Also, an adequate training should be provided to medical staff. Moreover, this is a requirement of the OHS legislation for all workplaces. Thus, it is established by the law that the employer shall "*identifies the risks specific to the conditions of epidemiological contamination and updates the risk assessment document for the safety and health of employees to the new conditions of activity, in order to take the necessary measures to combat the spread of SARS-CoV-2*" (Order no. 3577/831/2020). The necessary measures should be technical, administrative,

sanitary or by other types. However, they should be efficient in eliminating or reducing the risk and also they should be carefully designed so they not induce new risks. For example, providing masks for medical staff is a good measure, but a poor quality protection mask will make the measure to be inefficient. Also, providing UV lamps for sterilising the dental office is a good measure, but lack of worker training on how to use it in a proper way, will lead to occurrence of new serious risks for the health and safety of workers, such as skin burnings or eyes injuries.

In the context of COVID-19 pandemic, an important attention should be paid to the proper training of workers, based on the reviewed risk assessment. The training should be focused on issues as maintaining a proper personal hygiene, using correctly the PPEs (masks, protective shields, gloves, protective coverall) and the new equipment (*e.g.* UV sterilising lamp).

Also, a very important role is played by the OSH specialists (preventive and protective service, designated workers) who should be true counsellors for both the employer and the employees especially on the OHS issues raised by COVID-19 pandemic.

2. Risk Assessment Review in the Context of COVID-19 Pandemic

Identifying and assessing the OHS risks in a dental office was performed using the MEVA method for risk assessment, developed by National Research and Development Institute of Occupational Safety "Alexandru Darabont" Bucharest.

According to the method description, the first action performed by the assessment team is to describe the analysed system which is the workplace with its elements, respectively, operator, work task, means of production and work environment. These elements are described as follows:

- **Operator:** dentist. The assistant is considered to be another workplace, because even he/she operates in the same place with the dentist and they have some OHS risks in common, the work task is different, resulting a series of different risks for assistant comparatively with dentist.
- **Work task:** providing oral medical treatments for patients, treating diseases and other conditions that affect the teeth, gums and oral soft tissues, especially the repair and extraction of teeth and the insertion of artificial ones. The work task could be slightly different from case to case, depending on the specialisation level of the dentist. For a particular case, the work task should be described based on the job description document.

- **Means of production:** dental chair, dental sterilisers (autoclaves), handpieces, medical instruments, dental materials, drugs for dentistry, photopolymerisation lamp, ultrasonic scaler, Bunsen burner, gas boiler, UV-C sterilising lamp, dental office furniture (chairs, table, cabinets), power supply installation, water supply installation, natural gas supply, general lighting system.
- **Work environment** is characterised by the physical parameters, such as noise, vibrations, lighting, dusts, aerosols, temperature, humidity, air flows, ionising or non-ionising radiation and also by the biological parameters mainly determined by the specific health condition of the patients.

The following step of the method, identifying the risk factors of the system, is performed used a predefined list of general risks grouped on the elements of the work system. The level for each risk factor is established by the evaluation of two parameters, respectively, Probability (*P*) and Severity (*G*). *P* is established based on the evaluation of Frequency of Exposure (*F*) and Exposure Time Coefficient (*T*). *F* can have the values 1 (low), 2 (medium) or 3 (high) and it is evaluated based on the information collected by the assessment team from the workplace, including a compliance audit using specific checklists. *T* is established considering the estimated or calculated period of worker exposure to the risk, in relation with total shift time and can have the values as shown in Table 1 (Darabont *et al*., 2019).

Table 1
Exposure Time Coefficient (T)

T	**Percent of whole shift time**
1	0 – 20%
2	21 – 40%
3	41 – 60%
4	61 – 80%
5	81 – 100%

The possible values of P are shown in Table 2 and the possible values of G are shown in Table 3. The risk level is determined for each risk factor based on the values of P and G, using the Matrix for quotation of risk level, represented in Table 4. The Global Risk Level (Nrg) is calculated as a weighted mean of risk level values determined for all identified risk factors, using the following formula (Darabont *et al*., 2019):

$$Nrg = \frac{\sum_{i=1}^{n} r_i \cdot R_i}{\sum_{i=1}^{n} r_i} \quad (1)$$

where: R_i is the risk level determined for the risk factor *i*; r_i – weight for the risk factor i; by definition, $r_i = R_i$; *n* – number of identified risk factors.

Table 2
Quotation of Probability (P)

Probability (*P*)		**Values of Frequency of Exposure and Exposure Time Coefficient(*F,T*)**
1	Very Rare	(1,1) (1,2) (2,1)
2	Rare	(1,3) (1,4) (2,2) (3,1)
3	Less frequently	(1,5) (2,3) (3,2)
4	Frequently	(2,4) (2,5) (3,3)
5	Very frequently	(3,4) (3,5)

Table 3
Quotation of Severity (G)

Severity (*G*)		**Description**
1	Minor consequences	Reversible consequences, up to 3 days of work incapacity, no medical treatment needed
2	Medium consequences	Reversible consequences, 3-45 days of work incapacity, medical treatment needed
3	High consequences	Reversible consequences, 45-90 days of work incapacity, medical treatment needed
4	Serious consequences	Irreversible consequences, invalidity class 1 to 3 (diminishing work capacity by 50-100%)
5	Very serious consequences	Fatality

Table 4
Matrix for Quotation of Risk Level (R) and Safety Level (S)

R		***(G,P)***	***S***	
1	MINIMUM	(1,1) (1,2) (1,3) (2,1) (3,1)	5	MAXIMUM
2	LOW	(1,4) (1,5) (2,2) (2,3) (3,2) (4,1) (5,1)	4	HIGH
3	MEDIUM	(2,4) (2,5) (3,3) (4,2) (5,2)	3	MEDIUM
4	HIGH	(3,4) (3,5) (4,3) (4,4) (5,3)	2	LOW
5	MAXIMUM	(4,5) (5,4) (5,5)	1	MINIMUM

Using the MEVA method, the risks shown in Table 5 were identified and assessed considering the activity of a dental office before pandemic, without the OHS issues raised by the risk of infection with SARS-CoV-2.

Table 5
OHS Risks in Dental Office Before COVID-19 Pandemic

Work system element / Risk	***F***	***T***	***P***	***G***	***R***
Operator					
F1. Omission of using PPEs (e.g. respiratory protective mask, gloves, face shield) and work clothing (e.g. dentist coat, surgical cap, medical lab shoes).	1	1	1	4	2
F2. Hand injuries by improper handling of instruments.	1	1	1	2	1
F3. Hand injuries by improper handling of handpiece, burs and rotary attachments.	1	1	1	2	1

Work system element / Risk	*F*	*T*	*P*	*G*	*R*
F4. Injuries by hitting/crushing due to improper handling of furniture and equipment.	1	1	1	1	1
F5. Burns of the arms/hands due to improper handling of hot objects at instruments sterilising operations or improper operation of open flames.	1	1	1	2	1
F6. Injuries due to falls from the same level by slip, trip or loss balance.	1	1	1	2	1
F7. Injuries due to falls from low height (<2m) when accessing upper parts of the cabinets.	1	1	1	3	1
F8. Electrocution or exposure to electric arc due to unauthorised interventions to electrical equipment and installations.	1	1	1	5	2
F9. Traffic accidents during home-office trip or business trip, as pedestrian.	1	1	1	4	2
F10. Traffic accidents during home-office trip or business trip, as driver.	1	1	1	3	1
F11. Electrocution when performing authorised interventions and omitting to disconnect the equipment.	1	1	1	5	2
Work task					
F12. Lack of PPEs (e.g. respiratory protective mask, gloves, face shield) and work clothing (e.g. dentist coat, surgical cap, medical lab shoes) or poor quality of PPEs (e.g. masks without CE certification).	1	3	2	4	3
F13. Circulatory system diseases of lower limbs due to prolonged orthostatic/seated work position.	1	5	3	4	4
F14. Spine diseases due to awkward work position.	1	5	3	4	4
F15. Upper limbs diseases (of muscles, tendons, wrist, elbow, shoulder) by overloads at handling of the dental instruments.	1	5	3	4	4
F16. Additional physical effort due to unsuitable unit configuration to the laterality of the dentist (e.g. a left handed dentist working on a unit designed for right handed dentists).	1	5	3	3	3
F17. Mental effort (stress) due to difficulty of the interventions.	1	3	2	3	2
F18. Mental effort (stress) due to patient cooperation (child, difficult patients, patients with special needs etc.).	1	3	2	3	2
Means of production					
F19. Infection by accidentally contact with body fluids or tissue from patients with transmissible diseases, dentistry instruments and other materials with biological risk.	1	1	1	4	2
F20. Fire/explosion due to malfunctions of electrical devices or gas installation or equipment (e.g. gas boiler, Bunsen burner).	1	1	1	5	2

Work system element / Risk	*F*	*T*	*P*	*G*	*R*
F21. Fire/explosion due to accidentally contact of flammable substances or their vapours with open flames or hot surfaces.	1	1	1	5	2
F22. Hand skin rash or allergy by prolonged contact with latex gloves.	1	5	3	2	2
F23. Hand skin rash or allergy by direct contact with chemical products used in the dental office (e.g. cleaning, disinfection, sterilising, dental components and materials).	1	5	3	2	2
F24. Eyes rash or allergy by direct contact with chemical products used in the dental office (e.g. cleaning, disinfection, sterilising, dental components and materials).	1	1	1	2	1
F25. Injuries by hitting due to falling of objects (instruments, materials etc.).	1	1	1	2	1
F26. Hand injuries due to malfunctions of unit, dental office equipment, instruments etc.	1	1	1	2	1
F27. Hitting/crushing injuries due to malfunctions of furniture and equipment.	1	1	1	2	1
F28. Hands, face or eyes injuries due to break/detachment and throwing of objects or material fragments when using the handpiece.	1	1	1	4	2
F29. Injuries due to break/detachment and throwing of objects or material fragments from pressurised equipment.	1	1	1	5	2
F30. Exposure of hand to excessive vibration due to excessive wear or malfunctions of handpiece.	1	1	1	4	1
F31. Electrocution, exposure to electric arc or electrostatic discharge when using electrical equipment with malfunctions.	1	1	1	5	2
F32. Hands/arms burns by accidentally contact with hot pieces or with open flames.	1	1	1	2	1
F33. Injuries by falling of heavy objects or building elements in case of earthquake or calamity.	1	1	1	5	2
Work environment					
F34. Infection by exposure to solid/liquid particles in suspension in air (dust/aerosol) from the patients with transmissible diseases.	1	2	1	4	2
F35. Respiratory tract, skin or eyes allergy by direct exposure to dust, aerosol or vapours of chemicals (disinfection or sterilising products, dental materials).	1	4	2	2	2
F36. Visual fatigue due to improper lighting, attention to small details, using of magnifier.	1	4	2	2	2
F37. Illness by direct exposure to airflow or high/low temperatures in the office, without the possibility of optimising the temperature.	1	3	2	2	2
F38. Hearing loss due to prolonged exposure to noise generated by dental equipment.	1	4	2	4	3

Work system element / Risk	*F*	*T*	*P*	*G*	*R*
F39. Hearing damage due to prolonged exposure to ultrasounds generated by the ultrasonic scaler.	1	2	1	4	2
F40. Eyes damage due to exposure to optical radiation of photopolymerization lamp.	1	1	1	4	2
F41. Eyes damage due to exposure to UV-C radiation of the disinfection lamp.	1	1	1	4	2
F42. Illness of respiratory tract due to exposure to organic or mineral dust in suspension in air during tooth drilling operation.	1	5	3	3	3

Using formula (1), the Global Risk Level considering the activity of a dental office before pandemic (Nrg_A) has the value:

$$Nrg_A = \frac{\sum_{i=1}^{42} r_i \cdot R_i}{\sum_{i=1}^{42} r_i} = \frac{2 \cdot 2 + 1 \cdot 1 + 1 \cdot 1 + \cdots + 3 \cdot 3}{2 + 1 + 1 + \cdots + 3} = 2{,}28 \quad (2)$$

In the context of COVID-19 pandemic, the reviewed risk assessment for a dental office contain previously existing risks but with modified values for *R* and new risks determined by the potential exposure to SARS-CoV-2. Thus, the modified risks are represented in Table 6. Also, the new risks induced by COVID-19 pandemic are shown in Table 7.

Table 6

Modified OHS Risks in Dental Office in the Context of COVID-19 Pandemic

Work system element / Risk	*F*	*T*	*P*	*G*	*R*
Operator					
F1. Omission of using PPEs (e.g. respiratory protective mask, gloves, face shield) and work clothing (e.g. dentist coat, surgical cap, medical lab shoes).	1	1	1	5	2
Work task					
F12. Lack of PPEs (e.g. respiratory protective mask, gloves, face shield) and work clothing (e.g. dentist coat, surgical cap, medical lab shoes) or poor quality of PPEs (e.g. masks without CE certification).	1	5	3	5	4
Means of production					
F19. Infection by accidentally contact with body fluids or tissue from patients with transmissible diseases, dentistry instruments and other materials with biological risk.	1	5	3	5	4
Work environment					
F34. Infection by exposure to solid/liquid particles in suspension in air (dust/aerosol) from the patients with transmissible diseases.	1	5	3	5	4
F41. Eyes damage due to exposure to UV-C radiation of the disinfection lamp.	1	5	3	4	4

Table 7
New OHS Risks in Dental Office in the Context of COVID-19 Pandemic

Work system element / Risk	*F*	*T*	*P*	*G*	*R*
Means of production					
F43. Infection by directly contact with surfaces contaminated with SARS-CoV-2 (furniture, instruments).	1	5	3	5	4
Work environment					
F44. Infection by exposure to aerosol from patients and other persons with COVID-19.	1	5	3	5	4
F45. Infection by direct contact with patients and other persons with COVID-19.	1	5	3	5	4

Using formula (1), the Global Risk Level considering the activity of a dental office in the context of COVID-19 pandemic (Nrg_B) has the value:

$$Nrg_B = \frac{\sum_{i=1}^{45} r_i \cdot R_i}{\sum_{i=1}^{45} r_i} = \frac{2 \cdot 2 + 1 \cdot 1 + 1 \cdot 1 + \cdots + 4 \cdot 4}{2 + 1 + 1 + \cdots + 4} = 2{,}76 \quad (3)$$

The variation of Global Risk Level for the assessed dental office in the context of COVID-19 pandemic is Nrg_B - Nrg_A = 0.48 and is representing a grown of 21% comparatively with the Global Risk Level before pandemic (Nrg_A).

3. Considerations on the Measures to Prevent OSH Risks in the Context of COVID-19 Pandemic

The risk assessment reviewed in the context of pandemic should be completed with a series of specific preventive and protective measures aimed to prevent the risk of infection with SARS-CoV-2 for medical staff in the dental office. These preventive and protective measures should be applied in addition with previously established measures and should be technical, administrative and sanitary.

Technical measures. Examples of technical measures are the following:

– *Providing adequate PPEs to employees*. PPEs should include: masks, protective shields, gloves, protective coveralls. All PPEs must be CE certified. As regarding the masks, it cannot be considered that, for example, N95 or KN95 certified masks fulfil the CE requirements, unless a certification process was previously performed by a Notified Body. A CE certified mask is marked with “CE” mark followed by a four digits number representing the code of the Notified Body which performed the certification. Using this code, the Notified Body can be identified in the Nando list, available on the European Commission

website, at the following address: *https://ec.europa.eu/growth/tools-databases/nando/ index.cfm?fuseaction=notifiedbody.main*. Also, the Notified Body must be notified for PPEs certification. For example, National Research and Development Institute of Occupational Safety – INCDPM "Alexandru Darabont" is a Romanian Notified Body, having code 2756, notified for PPEs certification, on *Regulation (EU) 2016/425 Personal protective equipment*. Also, it is important to mention that the OHS specialists (internal/external preventive and protective service or designated workers) should advice the employer on selecting and purchasing adequate PPEs.

– *Providing UV-C lamps for sterilising the inner spaces.* These lamps should fulfil a series of technical requirements in order to be safe for users. For example, they should have a presence sensor to turn off the lamp in case of accidentally presence of a person in the room while the lamp is functioning and a remote control, to allow the operator to turn on/off the lamp from the outside of the room in which the lamp is functioning. Also, the lamps should have the adequate power density for an efficient sterilisation, considering the volume of the room.

Administrative measures. Examples of administrative measures are the following:

– *Filtering patients at the entrance in dental office*. The measure is intended to prevent the access of patients with COVID-19 symptoms.

– *Organising patients flows, with different routes for entry and exit.* Providing adequate and sufficient information for patients by signalisation, leaflets etc.

– *Providing proper training for workers* on subjects as: correct using of PPE, maintaining individual hygiene, correct using of UV-C lamps, periodic ventilation of the room and correct disposal of contaminated PPEs.

– *Avoid or prohibiting the aerosol-generating procedures*, especially when they are not a medical emergency (e.g. dental scaling).

Sanitary measures. For example:

– *Providing adequate disinfectants for hands and for surfaces.*

4. Conclusion

As any other professional activity, the activity performed by the medical personnel in dental offices involves OHS risks. The COVID-19 pandemic has induced significant changes in the structure and level of the OHS risks for all workplaces and particularly, for dental offices.

While some of the pre-existing risks have now a raised risk level due to pandemic, new risks appears in this context, determining important changes of the structure of workplace risks, value of Global Risk Level and the preventive

and measures necessary to be adopted by the employer in order to ensure the safety and protect the health of the workers.

An efficient prevention of the OHS risks raised by the COVID-19 pandemic requires a close collaboration of employer, workers and OHS specialists.

REFERENCES

American Dental Association, *OSHA Guidance Summary: Dentistry Workers and Employers* (online), 2020.

Darabont D.C., Smîdu E., Trifu A., Ciocîrlea V., Ivan I., Bejinariu C., Baciu C., Bernevig-Sava M.A., *MEVA - A New Method of Occupational Health and Safety Risk Assessment*, MATEC Web of Conferences, vol. **290**, p.12008, EDP Sciences, 2019.

Pece Șt., *Risk Assessment in the Work System*, Rubin Publishing House, Bucharest, 2010.

** Government Decision on Approving the Methodological Norms for Applying the Provisions of Occupational Health and Safety Law no.319/2006, no.1425/2006 with Subsequent Modifications and Completions, Official Gazette of Romania.

** Law of Occupational Health and Safety, no.319/2006, Official Gazette of Romania.

** Order no.3577/831/15.05.2020 of Ministry of Labour and Social Protection and of Ministry of Health.

RISCURILE SSM ÎN CABINETELE DENTARE ÎN CONTEXTUL PANDEMIEI DE COVID-19

(Rezumat)

Activitatea desfășurată de personalul medical din cabinetele dentare este caracterizată de riscuri specifice pentru securitatea și sănătatea în muncă (SSM), generate de echipamentele utilizate și de procedurile aplicate, precum și de unele aspecte de sănătate ale pacienților. O evaluare a riscurilor bine realizată este o condiție necesară pentru stabilirea măsurilor adecvate de prevenire și protecție și pentru a furniza lucrătorilor o instruire corespunzătoare. În plus, pandemia de COVID-19 a generat noi riscuri SSM pentru cabinetele dentare și a amplificat unele riscuri pre-existente. Lucrarea se orientează pe schimbările determinate de pandemie asupra riscurilor SSM și pe măsurile de prevenire și protecție necesar a fi adoptate pentru reducerea impactului acestor schimbări asupra personalului medical din cabinetele dentare.

BULETINUL INSTITUTULUI POLITEHNIC DIN IAŞI
Publicat de
Universitatea Tehnică „Gheorghe Asachi” din Iaşi
Volumul 66 (70), Numărul 1-4, 2020
Secţia
ŞTIINŢA ŞI INGINERIA MATERIALELOR

STUDY ON THE RUPTURE OF A NECK JOURNAL OF THE AXLE OF THE RETURN DRUM OF A BAND FEEDER IN THE CONSTRUCTION OF A HYDROCARBON PAVMENT MIXTURE PREPARATION PLANT. IDENTIFYING THE CAUSES OF THE EVENT

BY

GHEORGHE BĂDĂRĂU[1,*] and RODICA BĂDĂRĂU[2]

[1]“Gheorghe Asachi” Technical University of Iaşi,
Faculty of Materials Science and Engineering, Iași, Romania
[2]Politehnica University of Timișoara,
Faculty of Mechanics, Timișoara, Romania

Received: January 19, 2020
Accepted for publication: February 25, 2020

Abstract. The study presented in this paper discusses the causes that lead to an accidental rupture of a neck journal of the axel of the return drum of a feeding equipment placed at the input end of a rotating cylindrical dryer, both equipments being components of a complex installation destined for the preparation of hydrocarbon pavement mixtures. They are shown the importance of proper functioning of such equipment in the effort of ensuring at time materials for road construction field in great cities as a secondary key element in reducing air pollution. Starting from available initial data obtained during a previous study (Bădărău and Bădărău, 2018) and knowing the precise history of the feeding equipment operation problems, understanding that the same causes that, at a certain moment produced an unexpected extreme wear of the rubber band and the need for its replacement, and continuing chronologically with other elements, a certain course of events was established. They are listed in the form of a logical chain of argument, the objective causes and possible subjective causes that led to the failure occurrence. After identifying the type of rupture as

*Corresponding author; *e-mail*: gheorghe.badarau@tuiasi.ro

being produced by fatigue, elements sustaining a coherent scenario are given. Conclusions and some recommendations are focused on proposing ways of enhancing the machine reliability and better achievement of maintenance.

Keywords: equipment reliability; air pollution; objective and subjective cause of an event; faulty bearing slack; fatigue limit; tension adjustment.

1. Introduction

Among the multiple problems facing local authorities of big cities from Romania, the atmospheric pollution is brought more and more frequently into discussion by the nongovernmental organizations implied in this specific field. For example the Fundația Comunitară București attracts the attention that "the main causes of atmosphere pollution with PM10 and PM 2,5 in Bucharest are: road traffic (increasing number of existent cars in the capital: 1.3 million registered in October 2017, plus the cars that transit the city, plus those registered in other localities. These data lead to an estimation of over 2 million cars in traffic daily in the streets of the capital); pollution generated by buildings and construction sites that do not observe the rules of construction sites organization (lack of regulation concerning the control of such activities, abusive authorizations etc.); the increasingly acute lack of green spaces" (translated after - https://aerlive.ro/poluarea-aerului-in-bucuresti/).

It is easy to add, as an effect of a crowded traffic the reduction of the average transport speed in the city, growing of the combustible consumption because frequent stops and implicitly growing of pollution. The impact of the reduced average speed for transport is significant also in what concerns the economic activities from all points of view.

Another significant common cause of local pollution is urban planning, too many decisions taken in the last 20 years, which allowed the construction of large shopping centers inside the localities thus generating local concentration in the circulation of auto vehicles, especially of motorcars.

Solving these problems is, at least in theory difficult to achieve, because of the impact that is difficult for the population to accept. Inside the big cities with extended historical areas for example, traffic flow is often a difficult issue to resolve under the conditions of constraints related to the preservation of the architectural aspect and the conservation of the heritage: widening the streets being practically impossible.

The immediate remaining solution for historical areas is: the modernization, repair and maintenance of existing road infrastructure.

In the big cities of Romania This solution is being implemented as one of the priority objectives and at the same time one of the major challenges of the local administrations.

The concrete challenges related to this activity often consist in the proper execution of these road maintenance works, works that involve many specific constraints.

Among these can be mentioned those related to the actual time of existence of a construction site for a given artery, which is intended to be as short as possible, burdened by reduced labor productivity due to objective causes such as: work in the presence of traffic, therefore in conditions of high danger; work mainly at night, with an effect on overloading of workers and examples can continue.

In these conditions specific to road maintenance sites, ensuring the supply of materials is essential. The normal operation of all the equipment involved is also a condition without which a good result is unattainable.

Therefore, the operational safety of the equipment involved in the production of materials, transport and installation is a matter of significant importance and can be achieved only if maintenance is ensured properly (Smith, 2001; Smith and Hinchcliffe, 2004).

The paper aims to discuss the case of accidental rupture of a neck journal of the axle of the return drum of the feeding band (Răileanu *et al*., 2002; Simionescu *et al*., 1991; Simionescu *et al*., 1995), a very important component of a complex installation (Oprescu *et al*., 1997) namely of a hydrocarbon pavement mixture preparation plant.

It is desired to identify possible causes based on a set of available data collected about this rupture.

It is also desired to formulate a set of measures that can be considered recommendations for increasing the reliability of this machine.

2. Initial Data

Knowing the actual conditions under which a work equipment failure occurs is essential for formulating plausible assumptions about the possible causes capable of triggering such an event.

These conditions are always different from normal operation. In order to be able to highlight them, information is needed on the functional role of the part in the construction of the machine, on the working conditions of the machine as well as on its role in the installation of which it is part.

Once these elements have been clarified, it is possible to identify the type of strains to which the part is subjected under normal operating conditions and the value of these strains and then, implicitly, one can identify deviations from normal and which could become, in certain circumstances, causes of failures.

3. Machine Description and Overall Functional Role. History of Interventions

The band feeder, a machine in the category of conveyors with continuous operation, at which a neck journal of the axel of the return drum broke, is part of an installation for the production of hydrocarbon pavement mixtures, installation characterized by a maximum productivity of 150 t/h, with discontinuous operation, described in detail in the literature (Bădărău and Bădărău, 2018).

The machine feeds a dryer that has the role of precisely controlling the humidity of the granular mineral material (crushed or uncrushed sands, quarry or gravel sorters) that is part of the hydrocarbon pavement mixture.

The material to be dried also contains fine and very fine particles which, due to moisture, tend to adhere undesirably but significantly to the rubber conveyor belt of the feeder.

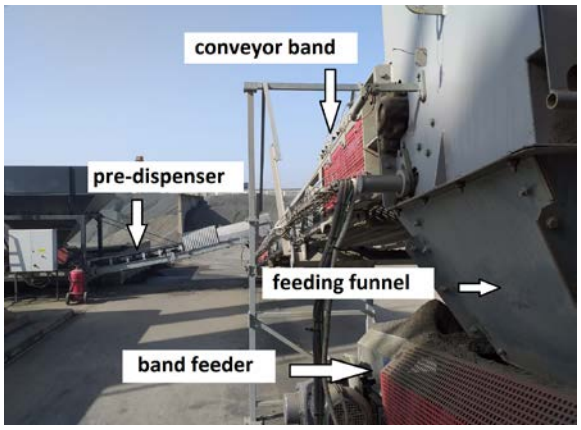

Fig. 1 – Pre-dosing and transport system of mineral material.

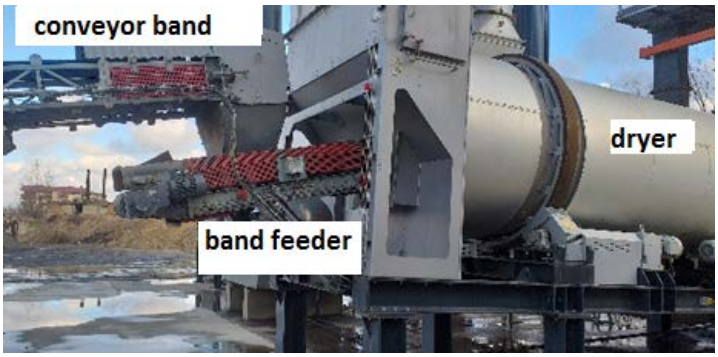

Fig. 2 – Position in the installation of the rubber band feeder (Bădărău and Bădărău, 2018).

In order to understand the place of the band feeder in the construction of the installation, we present the photos from Fig. 1 and Fig. 2 and as a detail the photograph from Fig. 3.

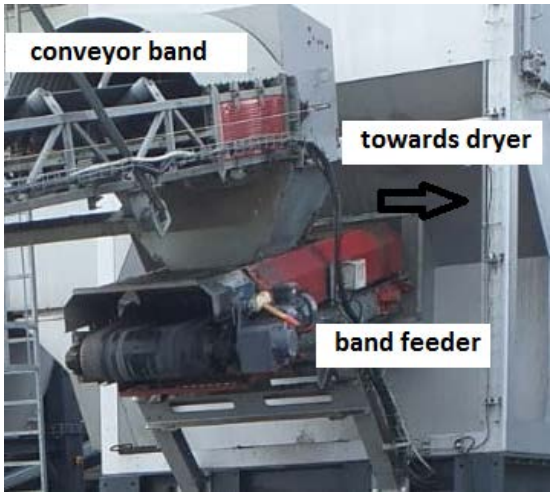

Fig. 3 – Position in the installation of the rubber band feeder. Detail (Bădărău and Bădărău, 2018).

In the case of this machine, in the past it was found that the extreme wear of the conveyor belt was caused by the lack of a safety part with a fixing role for the ball bearing, from the construction of one of the return drum bearings.

In a previous paper (Bădărău and Bădărău, 2018) there were described in detail the circumstances of the appearance and development of a severe defect, premature wear of the conveyor band, against the background of the tendency to move sideways by comparison with the normal direction of travel and the objective causes and possible subjective causes that produced it were described.

The intervention for the necessary replacement of the conveyor band, which lost about 10% of its width due to extreme wear, consisted of:

– dismantling the used band;

– finding the reason why the band feeder operated abnormal - a return drum bearing at which the assembly operations and assembly control did not meet the necessary quality conditions;

– disassembly of the return drum by removing the support bearings from the chassis;

– mounting a new bearing correctly equipped on the return drum;

– mounting on the equipment chassis the return drum equipped with a new bearing;

– installation of a new band on the conveyor;
– band tensioning, testing and commissioning of the machine.

4. Event Investigation

The observation of the operation of the equipment after the assembly of the new band on the conveyor and after the replacement of the return drum bearing was made carefully enough by the operating personnel, given the unwanted experience gained, which led to high repair costs and additional working hours required for intervention.

After a period of approximately 20 hours of use, an unjustified lateral movement of the rubber band on the return drum of the band feeder was again found.

This time it was intervened immediately by adjusting the conveyor band tensioner.

The lateral movement of the band, initially took place in the same part where its severe wear had previously occurred and then its misalignment became unstable, manifesting itself on both sides and could not be removed by adjustments, for an acceptable period of time.

At this point, specialized technical assistance was requested from the supplier.

The specialist assumed that the adhesions of material that are deposited on the return drum, in a too large quantity, are to blame for the bilateral, uncontrolled movement of the band. For removing this cause they came to the conclusion that the belt is not stretched enough.

The additional extension of the conveyor band by another 2 cm was the solution they adopted.

Following this additional adjustment, after a number of approximately 30 hours of operation, the return drum shaft broke near the neck journal corresponding to the newly mounted bearing.

It should be noted also, that the conveyor band resumed its tendency to deviate laterally from the normal direction of operation prior to this rupture, to the same part where the severe band wear had previously occurred, for an estimated duration of 10 hours.

5. Identification of the Type of Rupture and Preliminary Discussions

Identifying the type of rupture of a part made from a particular known material is important because it can provide clues about to the reasons for its occurrence.

Each type of material has a certain provision on behavior under strain, namely it has either a tenacious or a fragile behavior.

However, depending on the concrete circumstances in which a stress produces the rupture, the specific context consisting of: the value of the temperature, the dynamic of the stress, the presence in the environment of substances with corrosive effect etc. it is possible to change the natural behavior of a material from ductile to brittle.

The type of a rupture is visually identifiable, with the naked eye or under a microscope using different magnifying powers.

An advantage of such a study can be that of carrying it out shortly after rupture, so that the surface remains unaffected by corrosion, dust, dirt etc. thus allowing conclusions to be drawn with an increased degree of certainty.

The visual study of the rupture of the neck journal of the axle of the return drum was performed immediately after its disassembly from the machine chassis.

The disassembly was carried out immediately after the event in order to restore as soon as possible the production on the hydrocarbon pavement preparation plant. This helped very much to avoid corrosion on broken surfaces, the environment being humid.

Studying the surface resulted after the rupture of the neck journal of the return drum there were seen the classic signs of a fatigue fracture: waves, striae, the propagation area, the area of the final fracture, all of them visible on the both sides of the broken part Fig. 4. This kind of failure was considered a surprise taking into account the short duration of use for the return drum, about 1300 hours.

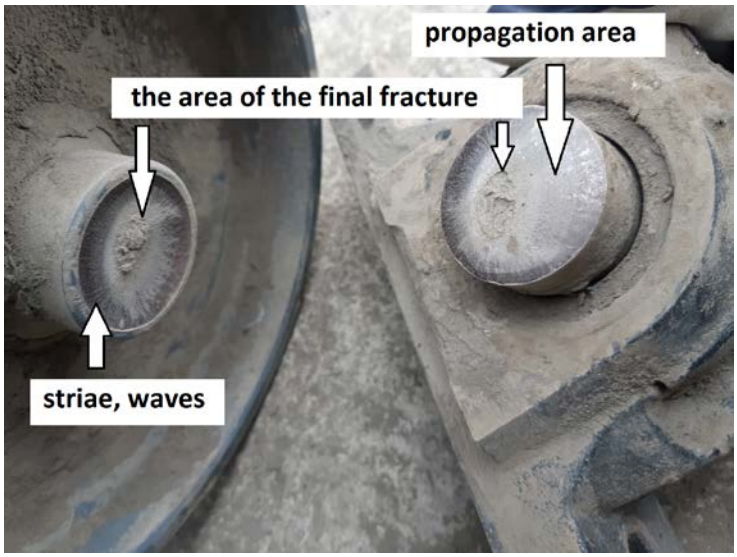

Fig. 4 – Rupture surfaces on the neck journal of the return drum of the feeding band: left side the return drum; right side the bearing containing a part of the neck journal.

Explaining such an event became a challenge in the context of previous experience with the same equipment.

The motive for an unexpected fatigue failure occurring is often provided by mistakes during designing of executing of parts subjected to cyclic stress components or/and by material problems.

For designing parts subjected to fatigue, the designer must take into account the macroscopic effects on the material behavior brought by: "of a simple, completely reversed alternating stress, a steady stress with a superposed alternating component, that is, the effects of cyclic stresses with a nonzero mean, alternating stresses in a multi axial state of stress, stress gradients and residual stresses, stress raisers, surface finish, temperature, humidity, corrosion and other environmental factors, size of structural element, accumulating cycles at various stress levels and the permanence of the effect, interaction between fatigue and other modes of failure" (Collins and Danilewicz, 2002).

In what concern the material quality, small defects and nonmetallic inclusions are usually to blame in specific conditions for fatigue failure (Murakami, 2002).

Accepting that generally, fatigue breakdown of a part can occur when the stress acting on it, produced by a certain load, has cyclic variations of various shapes or spectrums, finding these characteristics among causes become natural.

In this case, the theoretical load acting on the neck journal of the return drum can be considered as being produced by rotation bending. The value of bending load is given by the tension in the band that is adjusted with the tensioning system and by the transported material weight that can have fix or various values during operation whenever it is needed.

The torsion load can be easily considered very small, and can be neglected, because of the ball bearings mounted on both sides in the construction having the role of reducing friction.

In what concerns the shape of the loading cycle one can assume a combination of two types. Firth, a uniform sinusoidal load specific to the rotation of the return drum of the band feeder carrying continuously the mineral material needed, towards the dryer. Second, some changes made by the operator of the entire installation, meaning adjustments of the quantity of material supplied, meaning finally, variations in the rotation speed and load. This kind of stress, known as complicated stress spectrum is more dangerous than the other being hard to foreseen during designing. Usually, using safety coefficients when dimensioning, solves the problem. Nevertheless the time when such adjustment are being done is very small comparing to general operation. Its participation in the fatigue phenomenon is difficult to weight accurately for this specific case especially because it can consists in reducing stress, namely speed and load, and not only in enhancing them.

6. Identifying the Causes

For finding of the causes that produced the fatigue breakdown of a neck journal of the axle of the return drum one must necessarily take into account the mode of operation of the machine throughout the period of time until the occurrence of the rupture.

First of all, malfunctioning found during the unjustified lateral movement of the band feeder rubber band must not be forgotten. The causes that produced it can be common for both cases.

The major objective cause of malfunctioning of the band feeder was identified as: “an impermissible slack was found, caused by the lack of a spacer ring, for blocking movement (safety). This allowed the oscillation of the return drum along the axis on a variable length, with a maximum amplitude of about 3 mm” (Bădărău and Bădărău, 2018).

One can consider this sufficiently important for the neck journal fatigue breaking, only by seeing that a supplementary tension was induced by defectuous axial slack produced by the faulty bearing.

It is easy to assume that an axial slack of important amplitude produced vibrations during operation and another factor of accumulation of supplementary axial stress in the neck journal, and this could not be taken into account during designing.

Another possible cause, the additional stretching of the conveyor belt by another 2 cm, compared to the previous value, was the solution adopted by the specialists of the equipment supplier in an attempt to remove the effect of lateral displacement of the band. Mentioning that the previous adjustment of the tension was made without any indications completes the image.

The supplementary force applied in this way on the neck journals of the axel worked probably as a significant overload. This motive was already identified as a second objective cause through the fault of the manufacturer of the equipment, in the category - “failure due to operating documentation” (Smith, 2001), “namely the lack of technical documentation about the values indicated for tensioner adjustment” (Badarau and Bădărău, 2018).

Another question to ask is about the possibility of remarking signs of cracks or micro cracks before the fracture on the neck journal, during the remediation operation that consisted in the replacement of the rubber band.

Answering this questions lead us towards the discussion on two scenarios:

– there were no cracks on the surface;

– even if there were any cracks on the neck journal, they were not large enough to be seen (lack of specific instruments - at least a magnifying glass) or, more probably they could not be seen because of the dirty surface.

Because there are no sufficient evidence about this problem a recommendation must be made in what concerns the maintenance procedure: to carefully check the integrity of used parts before reassembling.

Nevertheless the reoccurring of the displacement of the band relatively soon after the remediation of the bearing can be put now, more probable on an existent micro crack of the neck journal that evolved in relatively short time.

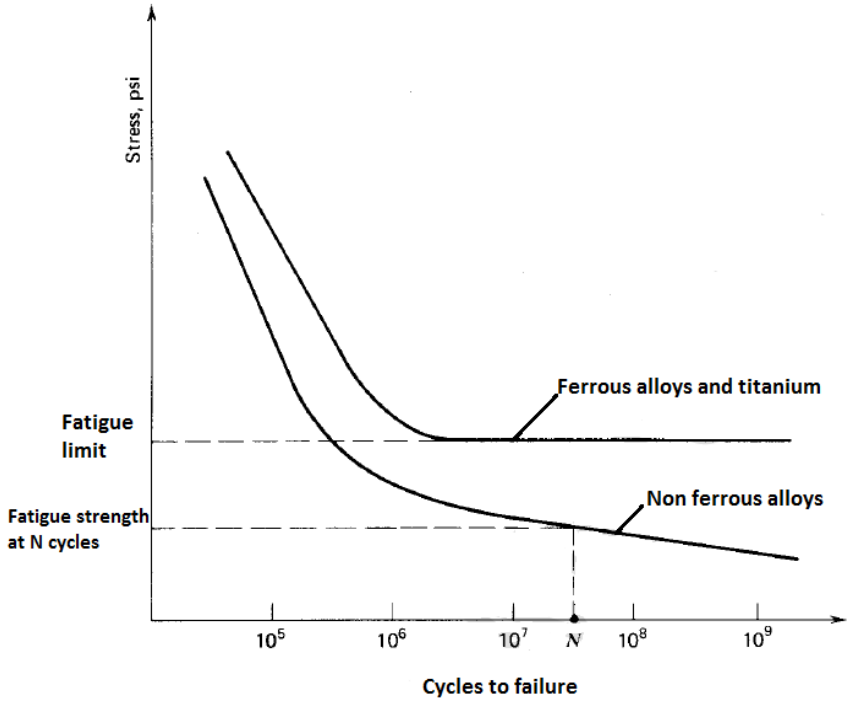

Fig. 5 – Fatigue limit vs cycles to failure (Collins and Danilewicz, 2002).

The growing of some micro cracks and their rapid transformation in fatigue cracks was helped by the repeated attempts to adjust the band position using more and more tension, finally overpassing the stress representing the fatigue limit, Fig. 5.

It was the moment when the displacement of the band started to oscillate toward right and left without the possibility of adjustment.

In this moment more tension has been added and the number of hours to complete failure was about 10 h corresponding to approximated 82000 rotation cycles, that is consistent with the general values for steel, Fig. 5 and Fig. 8.

Going further with the investigation one can discover some issues about the shape and about the technology of the return drum itself.

The return drum is made from steel by welding a calendric part with two caps having through holes at the diameter of the axle. The axle is welded by the caps and the ensemble is painted partly in blue.

All the parts are being made using a lathe type machine from laminated semi products: pipe for the cylindrical part, sheet for the caps and rod for the axle Fig. 6.

Fig. 6 – Return drum with bearing – left side. Detail of axle neck journal - right side.

The axel technology involves before welding, a longitudinal turning operation and the neck journal is cut from a laminated semi product. The roughness level of the neck journal is surprisingly high taking into account the bearings mounted on it. Careless longitudinal turning can be seen also exactly were the fracture took place, a sharp edge (stress raiser) between the two diameters, instead of a radius.

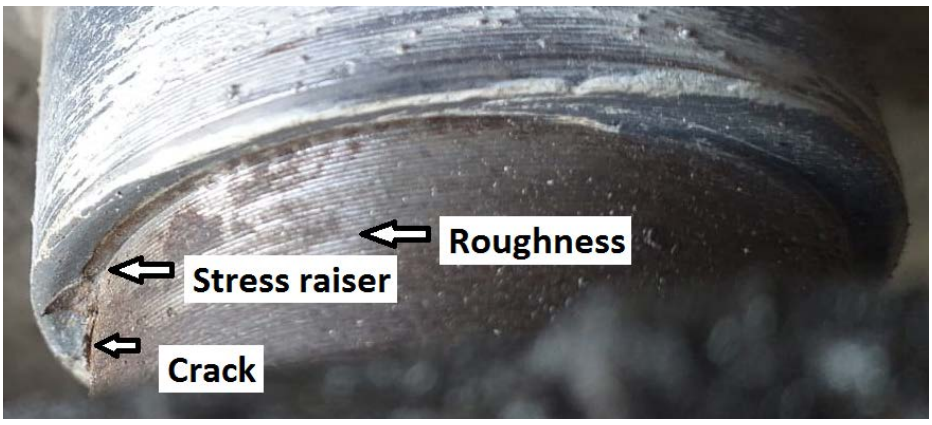

Fig. 7 – Details presenting the stress raiser and the roughness of the surface of the neck journal.

The sharp edge let after cutting is a source of micro cracks as well as the roughness of the surfaces and the recommendations for designers are to avoid them when fatigue is probably to be involved during operation of a part.

By consequence, the presence of an obvious stress raiser, the sharp edge, can be taken into account as another objective cause of failure identified for the fatigue breaking of the neck journal Fig. 7.

An apparent crack can be seen on the picture, but an attentive verification confirmed that, it extent is only at the paint level and does not enter inside the material.

The welding technology used for the return drum construction suggests the use of low carbon steel, the fatigue limits being given in Fig. 8.

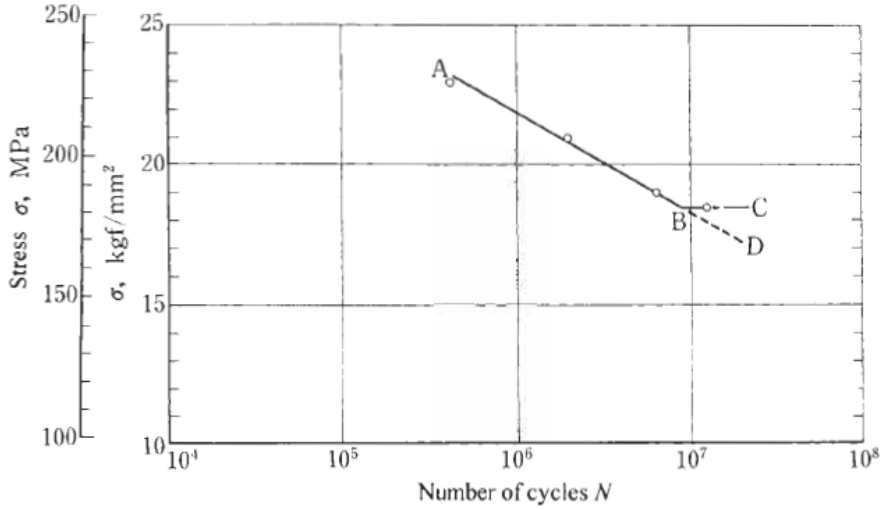

Fig. 8 – S-N curve for a low carbon steel (Collins and Danilewicz, 2002).

7. Conclusions and Recommendations

The defectuous construction of a bearing installed on a rubber band feeder return drum produced a severe wear of the conveyor band that required its replacement, in the first stage of deployment, led to the progressive misalignment of the rubber band and improper operation of the machine.

After repair and re-commissioning, in a relatively short time, about 40 hours, the problems of adjusting the band position reappeared, most likely due to the opening of a fatigue crack.

The additional extension of the band, used in the intention of readjusting the position, led to exceeding the fatigue resistance limit of the neck journal material (steel) and a number of only 10^4 rotation cycles was sufficient until the rupture occurred.

The causes identified for the fatigue breakdown of the part in discussion are:

– presence of a stress raiser in the shape of a sharp edge obtained during cutting the neck journals of the return drum axle, by turning;

– supplementary stress, added for a period of time, in form of an axial load not taken into account in the design (stress due to axial slack);

– at some point the load due to repeated tensioning attempts has overcame the fatigue strength limit, specific to the material from which the axle was made.

In order to accurately identify all the conditions that led to the breaking of the part, additional investigations on the material are needed and will be conducted.

It is recommended to correct the shape of the part, namely the sharp edge, present in the current design of the neck journal and transform it using a radius for avoiding the stress raiser and also a reduction of the roughness in the same area is advisable.

It becomes imperative to ask the equipment supplier for very clear instructions regarding the band tension adjustment procedure.

It is strongly recommended as a maintenance procedure to avoid reusing parts that have worked in conditions, other than those for which they were designed and, in exceptional cases, when they cannot be replaced with new parts, it is necessary to check them very carefully.

REFERENCES

Bădărău R., Bădărău Gh., *Study on the Exterme Wear of the Conveyor Band of a Rubber Band Feeder in the Construction of a Hydrocarbon Pavment Mixture Preparation Plant. Identifying the Causes of the Event*, Bul. Inst. Polit. Iaşi, s. Materials Science and Engineering, **64 (68)**, *1-4*, 43-53 (2018).

Collins J.A., Danilewicz S.R., *Chapter 25 Failure Modes: Performance and Service Requirements for Metals, pag. 722-740, in *** Handbook of Materials Selection*, John Wiley & Sons., 2002

Murakami Y., *Metal Fatigue: Effects of Small Defects and Nonmetallic Inclusions*, Elsevier Science Ltd., 2002.

Oprescu I., Vîrcolacu I., Gheorghiu F., Bălescu C., Guțu M., *Utilaje metalurgice*, Editura Didactică și Pedagocică, București, 1977.

Răileanu T., Mirea C., Grancea V., Bădărău Gh., Cucoș I., *Utilaje și mașini pentru pregătirea amestecurilor de formare*, Editura "Gh. Asachi" Iași, 2002.

Simionescu A., Raileanu T., Nejneru C., Hegyi E., Bădărău Gh., *Utilaje metalurgice specifice. Îndrumar de laborator*, Universitatea Tehnică "Gh. Asachi" Iaşi, 1995.

Simionescu A., Scânteianu N., Nejneru C., Ioniță I., Grancea V., Hegyi E., *Utilaje metalurgice specifice, Îndrumar de proiectare, Utilaje de transport cu funcționare continuă*, Institutul Politehnic "Gh. Asachi" Iaşi, 1991.

Smith D.J., *Reliability, Maintainability and Risk. Practical Methods for Engineers, Sixth Edition*, Butterworth – Heinemann Ltd, Linacre House, Jordan Hill, Oxford, UK, 2001.

Smith A.M., Hinchcliffe G.R., *RCM – Gateway to a World Class Mentainance*, Elsevier Butterworth – Heinemann, Linacre House, Jordan Hill, Oxford, UK, 2004.

https://aerlive.ro/poluarea-aerului-in-bucuresti/

STUDIU PRIVIND RUPEREA UNUI FUS AL AXULUI TAMBURULUI DE ÎNTOARCERE AL UNUI ALIMENTATOR CU BANDĂ DE CAUCIUC DIN CONSTRUCȚIA UNEI INSTALAȚII DE PREPARARE A MIXTURILOR ASFALTICE. IDENTIFICAREA CAUZELOR EVENIMENTULUI

(Rezumat)

Studiul prezentat în această lucrare discută cauzele care au dus la o rupere accidentală a unui fus al axului tamburului de întoarcere al unui alimentator plasat la intrarea într-un uscător cilindric rotativ, ambele echipamente fiind componente ale unei instalații de preparare a mixturilor asfaltice. Sunt arătate importanța funcționării corespunzătoare a unor astfel de echipamente în efortul de a asigura la timp materiale în domeniul construcției de drumuri în marile orașe ca element cheie secundar în reducerea poluării atmosferice. Pornind de la datele disponibile dintr-un studiu anterior (Bădărău and Bădărău, 2018) și cunoscând precis istoricul problemelor de funcționare ale alimentatorului, înțelegând că aceleași cauze, care la un anumit moment au produs uzura extremă a benzii de transport din cauciuc și nevoia înlocuirii ei, și continuând cronologic cu alte elemente, a fost stabilit un anumit curs al evenimentelor. Sunt enumerate în forma unui lanț logic argumentat cauzele obiective și posibilele cauze subiective care au condus la apariția ruperii. După identificarea tipului de rupere ca fiind rupere prin oboseală, sunt date elementele care susțin un scenariu coerent în acest sens.

Concluziile și recomandările sunt concentrate pe propunerea de modalități de a crește fiabilitatea utilajului și de realizare în condiții mai bune a mentenanței.

BULETINUL INSTITUTULUI POLITEHNIC DIN IAŞI
Publicat de
Universitatea Tehnică „Gheorghe Asachi” din Iaşi
Volumul 66 (70), Numărul 1-4, 2020
Secţia
ŞTIINŢA ŞI INGINERIA MATERIALELOR

ANALYSIS OF CONTACT ANGLE FOR DIFFERENT TYPE OF COATINGS

BY

DIANA-PETRONELA BURDUHOS-NERGIS, DUMITRU-DORU BURDUHOS-NERGIS and COSTICĂ BEJINARIU*

“Gheorghe Asachi” Technical University of Iaşi,
Faculty of Materials Science and Engineering, Iaşi, Romania

Received: October 5, 2020
Accepted for publication: November 18, 2020

Abstract. Corrosion is one of the most common phenomena that lead to the decommissioning of steel parts. Over time, attempts have been made to continuously improve the corrosion resistance of various types of steel. Therefore, coatings are one of the most important technologies for improving the corrosion resistance of metals. There are many methods of protection of steel against corrosion, such as: organic coatings, metal coatings, pretreatments etc. However, one of the most used methods is phosphating. In this paper, the value of the contact angle was determined in order to evaluate the degree of wetting of four types of samples (carbon steel, phosphate carbon steel, phosphate and painted carbon steel and phosphate and lubricated carbon steel).

Keywords: carbon steel; contact angle; phosphating process; lubricant; paint.

1. Introduction

Nowadays, the field of coatings for improving corrosion resistance is given a much more importance. Many researchers study the corrosion mechanism and the properties of the traditional coatings (Cunha *et. al.*, 2008;

*Corresponding author; *e-mail*: costica.bejinariu@tuiasi.ro

Ernens *et al.*, 2018). Also, due to the environmental issues, new coatings are developed and analyzed (Kalidindi and Subasri, 2015).

Among the most well-known and used methods of protection against corrosion is phosphating. The phosphating process consists essentially in the formation on the metal surface of a protective film of insoluble phosphates (Burduhos-Nergis *et al.*, 2019a). The phosphate film exerts its anti-corrosion protective role in combination with other films subsequently deposited on it: varnishes, paints, oils. Subsequent deposition of such a layer is favored by the porous structure of the phosphate layer and its absorbent properties (Abdalla *et al.*, 2014).

It is known that the coating layers deposited by conversion on metal surfaces, involving chemical precipitation processes with the formation of hard soluble compounds and strongly adherent to the substrate, have physico-chemical and mechanical properties depending on surface architecture, nature of materials and coating technology parameters (Duszczyk *et al.*, 2018).

The layers obtained by phosphating are used, due to the fact that these films have special characteristics: corrosion protection, substrate for painting and impregnation, solid lubricant in the process of cold deformation of metals, aesthetic role (polychromes) etc.

Phosphating is the most widely used metal pretreatment process for surface treatment and finishing of ferrous and non-ferrous metals (Etteyeb *et al.*, 2006). Due to its accessibility, speed of application and ability to allow excellent resistance to corrosion, wear and adhesion, it plays a significant role in the automotive industry (Fernandes *et al.*, 2011).

Although the process was originally developed as a simple method to prevent corrosion, the end uses of phosphate parts have forced the modification of existing processes and the development of innovative methods to replace conventional ones (Hafiz *et al.*, 2008). In order to keep pace with the rapidly changing needs of finishing systems, numerous changes have been made to both the processing sequence and the content of phosphating solutions.

Considering the importance of the phosphating process, the present paper aims to determine the contact angle for evaluating the degree of wetting of four types of samples: carbon steel, phosphate carbon steel, phosphate and painted carbon steel and phosphate and lubricated carbon steel.

2. Materials and Methods

The base material used in this study is carbon steel, C45, on the surface of which a zinc-based phosphate layer was deposited by conversion. After phosphating, a number of samples were selected on the surface of which a layer of elastomer-based paint was deposited by spraying or were impregnated for 5 minutes in a molybdenum bisulfide-based lubricant.

Contact angle measurement is a method used to describe the hydrophobic or hydrophilic behavior of a material. It provides information on the wettability of a surface by measuring the angle of contact between a liquid and a solid formed at the gas-liquid-solid interface. This is determined geometrically by drawing a tangent from the point of contact along the gas-liquid-solid interface, as shown in is shown in Fig. 2.18 (Gu *et al.*, 2016).

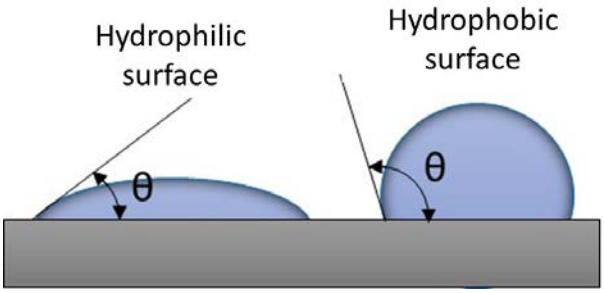

Fig. 1 – Contact angle measurement.

The value of the contact angle (θ) formed by a drop of liquid deposited on a smooth surface is greater than 90° if the affinity between liquid and solid is low; in the case of water, the material is considered hydrophobic, and if the angle is less than 90°, the material is considered hydrophilic (Fig. 1). Humectation occurs at 0°, when the liquid spreads on the surface (Chau, 2009).

The contact angle was measured using the static method of the liquid drop on a flat surface using the Easy Drop Kruss equipment with Drop Shape Analysis software. The four liquids (rainwater, distilled water, Black Sea water and fire extinguishing solution) were applied to the flat surface of the 10 mm diameter and 3mm high cylindrical sample using an 8 microliter microsyringe. 5 measurements were performed in order to measure the static contact angle, which allowed the determination of a mean value for each sample and each type of wetting agent. As far as the dynamic contact angle is concerned, 15 measurements were performed for 30 seconds on each sample.

3. Results and Discussions

The value of the contact angle was determined in order to evaluate the wetting degree of the C45 steel, of the initial zinc phosphate layer (C45F), painted (C45FV) and lubricated (C45FU).

The value of the contact angle depends on the chemical composition of the solid, the wetting agent and the surface roughness.

The mean value of the contact angles measured using the static method for each sample is shown in Table 1.

Table 1
Average Values of the Contact Angle

Sample	C45	C45F	C45FU	C45FV
Liquid	Rainwater			
Contact angle (degrees)	103.5	75.9 (65.6)	84.6	82
Liquid	Distilled water			
Contact angle (degrees)	106.9	75.9 (52.7)	120.8	87.3
Liquid	Black Sea water			
Contact angle (degrees)	100.6	66.3	-	84.4
Liquid	Fire extinguishing solution			
Contact angle (degrees)	79.9	64.7	157	60.4

As one can see, the value of the contact angle for carbon steel is higher than 90º when rainwater, distilled water and Black Sea water are used as wetting agents, as it has a hydrophobic nature. Due to the viscosity of the fire extinguishing solution, the value of the contact angle for the C45 decreases, while its moisture content increases. The contact angle images for the C45 sample are shown in Fig. 2.

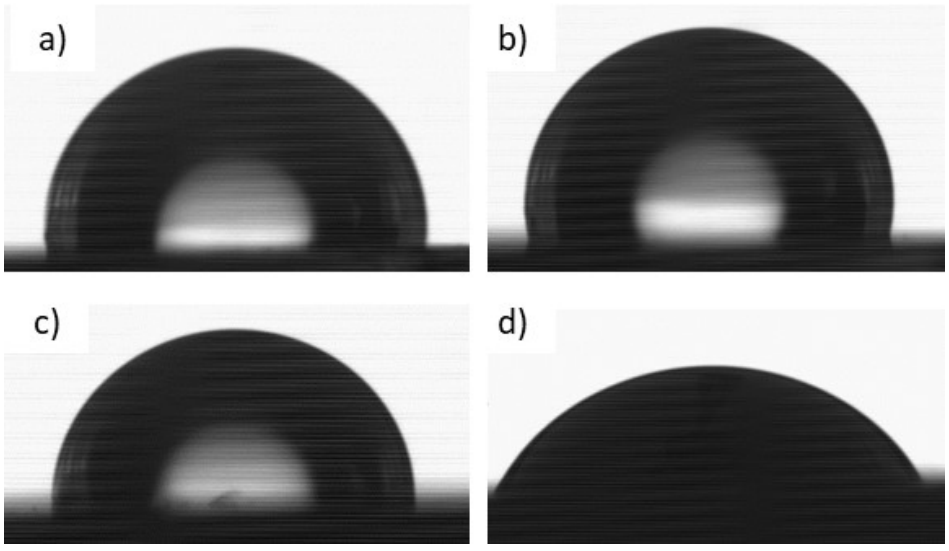

Fig. 2 – Contact angle for the surface of the C45 steel sample using wetting agents: *a*) rainwater; *b*) distilled water; *c*) Black Sea water; *d*) fire extinguishing solution.

The deposition of a crystalline coat of insoluble phosphates on the surface of the steel increases the porosity of the surface. Studies have shown that the roughness of the material is inversely proportional to the value of the contact angle. Therefore, the roughness of the zinc phosphate coat influences the value of the contact angle, which is less than 90º for all wetting agents, the sample having a hydrophilic nature. Fig. 3 shows the drop deposited on the coat surface.

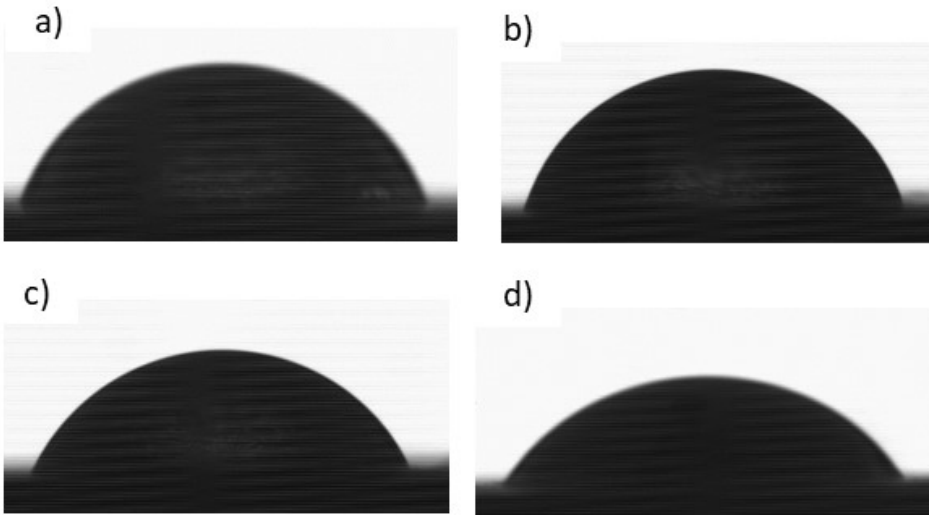

Fig. 3 – Contact angle for the surface of the zinc phosphate layer using wetting agents: *a*) rainwater; *b*) distilled water; *c*) Black Sea water; *d*) fire extinguishing solution.

The contact angle values for the C45 zinc phosphate-coated steel sample confirm the results of the scratch test (Burduhos-Nergis *et al*., 2019b). The porous surface of the coat allows its impregnation with lubricant or the deposition of an elastomer-based paint.

Contact angle measurements were also performed for the phosphate-coated sample impregnated with molybdenum disulfide lubricant. Due to the increase in the value of the contact angle for all wetting agents, the drop flowed too quickly from the surface of the sample, so no image of it was recorded. This is due to the ability of water molecules to diffuse into the structure of the phosphate coat.

As shown in Fig. 4, the deposition of a coat of paint after phosphate covering increased the value of the contact angle by about 10º, for all water types. The roughness of the surface, created by paint particles, determines the hydrophilic nature of the sample.

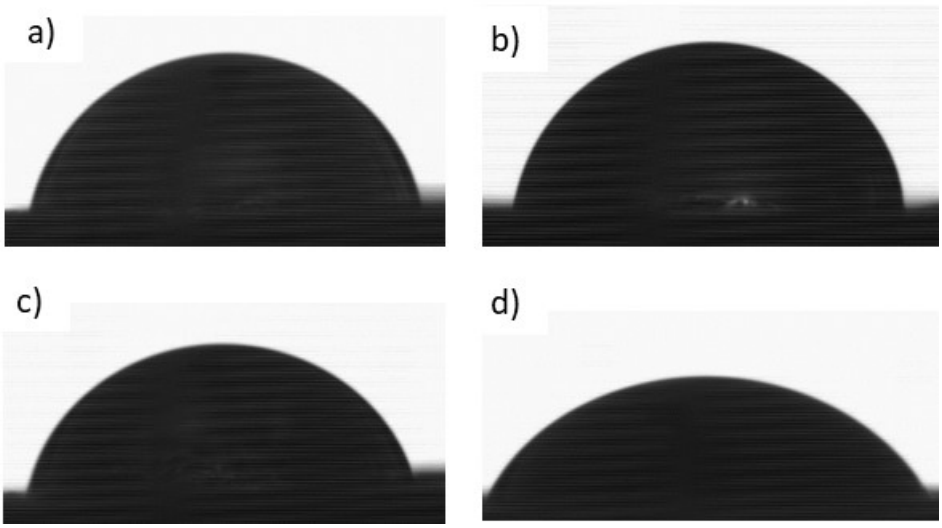

Fig. 4 – Contact angle for the painted surface using wetting agents:
a) rainwater; *b*) distilled water; *c*) Black Sea water; *d*) fire extinguishing solution.

The non-phosphate-coated sample showed a hydrophobic nature when in contact with the various water types, while the phosphate-coated painted one showed a hydrophilic nature. By impregnating the phosphate-coated samples in molybdenum disulfide lubricant, their nature becomes hydrophobic.

4. Conclusions

The non-phosphate-coated sample exhibited a hydrophobic nature when in contact with the types of water (rainwater, Black Sea water and distilled water) studied, and the painted phosphate-coated one exhibited a hydrophilic nature. By impregnating the phosphate-coated samples in molybdenum disulfide lubricant, their nature becomes hydrophobic.

REFERENCES

Abdalla K., Rahmat A., Azizan A., *Influence of Activation Treatment with Nickel Acetate on the Zinc Phosphate Coating Formation and Corrosion Resistance*, Materials and Corrosion, **65**, 977-981, 2014.

Burduhos Nergis D.P., Nejneru C., Burduhos Nergis D.D., Savin C., Sandu A.V., Toma S.L., Bejinariu C., *The Galvanic Corrosion Behavior of Phosphated Carbon Steel Used at Carabiners Manufacturing*, Revista de Chimie, **70**, 215-219 (2019a).

Burduhos-Nergiș D.P., Cimpoesu N., Vizureanu P., Baciu C., Bejinariu C., *Tribological Characterization of Phosphate Conversion Coating and Rubber Paint Coating Deposited on Carbon Steel Carabiners Surfaces*, Materials Today: Proceedings, **19**, 969-978 (2019b).

Chau T.T., *Membrane Contactors: Fundamentals, Applications and Potentialities*, Minerals Engineering, **22**, *3*, 213-219 (2009).

Cunha C.A, Lima N.B, Martinelli J.R, Bressiani A.H.A., Padial A.G.F., Ramanathan L.V., *Microstructure and Mechanical Properties of Thermal Sprayed Nanostructured Cr3C2–Ni20Cr Coatings*, Mat. Res., **11**, *2*, 137-143 (2008).

Duszczyk J., Siuzdak K., Klimczuk T., Strychalska-Nowak J., Zaleska-Medynska A., *Manganese Phosphatizing Coatings: The Effects of Preparation Conditions on Surface Properties*, Materials, **11**, *12*, 2585 (2018).

Ernens D., de Rooij M.B., Pasaribu H.R., van Riet E.J., van Haaften W.M., Schipper D.J., *Mechanical Characterization and Single Asperity Scratch Behaviour of Dry Zinc and Manganese Phosphate Coatings*, Tribology International, **118**, 474-483 (2018).

Etteyeb N., Sanchez M., Dhouibi L., Alonso C., Andrade C., Triki E., *Corrosion Protection of Steel Reinforcement by a Pretreatment in Phosphate Solutions: Assessment of Passivity by Electrochemical Techniques*, Corrosion Engineering Science and Technology, **41**, 336-341 (2006).

Kalidindi R.S.R., Subasri R., *Sol-Gel Nanocomposite Hard Coatings, in Anti-Abrasive Nanocoatings. Anti-Abrasive Nanocoatings*, Woodhead Publiching, 105-136, ISBN: 978-0-85709-211-3, Cambridge, United Kingdom, 2015.

Fernandes K.S., Alvarenga E.A., Brandao P.R.G., Lins V.F.C., *Infrared-Spectroscopy Analysis of Zinc Phosphate and Nickel and Manganese Modified Zinc Phosphate Coatings on Electrogalvanized Steel*, R. Esc. Minas, **64**, *1*, 45-49 (2011).

Gu H., Wang C., Gong S., Mei Y., Li H., Ma W., *Investigation on Contact Angle Measurement Methods and Wettability Transition of Porous Surfaces*, Surface and Coatings Technology, **292**, 72-77 (2016).

Hafiz M.H., Kashan J.S., Kani A.S., *Effect of Zinc Phosphating on Corrosion Control for Carbon Steel Sheets*, Eng. & Technology, **26**, *5*, 501-511 (2008).

ANALIZA UNGHIULUI DE CONTACT PENTRU DIFERITE TIPURI DE ACOPERIRI

(Rezumat)

Coroziunea este unul dintre cele mai frecvente fenomene care duc la scoaterea din uz a pieselor din oțel. De-a lungul timpului, s-a încercat îmbunătățirea continuă a rezistenței la coroziune a diferitelor tipuri de oțel. Prin urmare, acoperirile sunt una dintre cele mai importante tehnologii pentru îmbunătățirea rezistenței la coroziune a metalelor. Există multe metode de protecție a oțelului împotriva coroziunii, cum ar fi: acoperiri organice, acoperiri metalice, pretratamente etc. Cu toate acestea, una dintre

cele mai utilizate metode este fosfatarea. În această lucrare, valoarea unghiului de contact a fost determinată pentru a evalua gradul de umectare a patru tipuri de probe (oțel carbon, oțel carbon fosfatat, oțel carbon fosfatat și vopsit, precum și oțel carbon fosfatat și impregnat în lubrifiant).